Electromagnetic mass differences of pions and kaons

John F. Donoghue
Department of Physics and Astronomy, University of Massachusetts, Amherst, Massachusetts 01003

Antonio F. Pérez
Department of Physics and Astronomy, University of Massachusetts, Amherst, Massachusetts 01003
and Department of Physics, University of Cincinnati, Cincinnati, Ohio 45221
(Received 9 December 1996)

We use the Cottingham method to calculate the pion and kaon electromagnetic mass differences with as few model-dependent inputs as possible. The constraints of chiral symmetry at low energy, QCD at high energy, and experimental data in between are used in the dispersion relation. We find excellent agreement with experiment for the pion mass difference. The kaon mass difference exhibits a strong violation of the lowest order prediction of Dashen's theorem, in qualitative agreement with several other recent calculations. [S0556-2821(97)05309-5]

PACS number(s): 13.40.Dk, 12.39.Fe

I. INTRODUCTION

The calculation of the electromagnetic (EM) mass differences of pions and kaons has recently been quite an active topic [1–5] in the field of chiral perturbation studies. This is partially due to the interest in the values of the light quark mass ratios, for which we need to be able to separate electromagnetic from quark mass effects [6–8]. The realization that Dashen's theorem [9], relating pion and kaon electromagnetic mass differences in the limit of vanishing m_u, m_d, m_s, could be significantly violated in the real world [3–5,10] has added to the importance of a direct calculation of these electromagnetic effects. Moreover, these calculations have an intrinsic interest as state of the art investigations of our ability to handle new types of chiral calculations. The classic studies of chiral perturbation theory [11,12] are being extended to calculations where one must obtain more detailed information of the intermediate energy region using dispersion relations (or sometimes models). The electromagnetic mass differences are nonleptonic amplitudes which are a challenge to calculate in a controlled fashion. It is our goal in this paper to calculate these mass differences as well as we can at present.

Our tool is the Cottingham method for calculating electromagnetic mass differences. As explained more fully in Sec. III, this converts the mass difference amplitude into a dispersion integral over the amplitudes for $\gamma\pi$ inelastic scattering. As we learned in the 1970s from the study of γp inelastic scattering, the physics of such a process is reasonably simple. The elastic scattering is well known. At low energies, one sees the inelastic production of the low-lying resonances. In our study we take these resonances and their coupling constants from experimental data. At high energies one enters the deep inelastic region for which perturbative QCD can be used. It turns out that in the pion mass difference the deep inelastic region cancels out both at zeroth and first order in the quark masses. This leaves the mass differences to be dominated by the lower energy region.

There are a series of constraints on the calculation which are important for giving us control over our method and results. The most important of these are the following.

(1) There exists a rigorous result for these mass differences, exact in the limit that $m_q \to 0$, $(q = u,d)$ which states that in this chiral limit the pion mass difference is

$$\Delta m_\pi^2 = -\frac{3\alpha}{4\pi F_\pi^2}\int ds\, s\, \ln[\rho_V(s) - \rho_A(s)], \qquad (1)$$

where $\rho_V(s)$ and $\rho_A(s)$ are the vector and axial-vector spectral functions measured in e^+e^- annihilation and in τ decays [13]. This is a powerful constraint because it requires that the full calculation differs from this only by terms of order m_π^2 or higher, and must reduce to this as $m_\pi^2 \to 0$. Many of these deviations are kinematic in origin and hence are well tied down by this constraint.

(2) Dashen's theorem states that in an SU(3) extension of this same limit $m_q = 0$, $(q = u,d,s)$ that the kaon mass difference is equal to the pion mass difference. This means that similar physics enters both amplitudes and one is able to focus more directly on SU(3) breaking.

(3) The low energy structure of the Compton amplitudes $\gamma\pi \to \gamma\pi$ and $\gamma K \to \gamma K$ are known rigorously from chiral perturbation theory [14–17] and the process in the crossed channel $\gamma\gamma \to \pi\pi$ matches well with experiment [17].

(4) QCD gives us important information about the high energy behavior of the dispersive integral, with the result that Δm_π^2 is finite up to order m_q^2, while Δm_K^2 has at most a logarithmic divergence at order m_q, which is to be absorbed into the u,d quark masses. This is very useful in pinning down the high energy parts of the calculation.

(5) The medium energy intermediate states are known directly from experiment. This region is the most difficult to control purely theoretically, and so we rely on experimental data to overcome our inability to provide a first-principles theoretical calculation.

These properties are important ingredients for the reliability of our method. While there are still some approximations and educated guesses involved in the matching up of the various regions of the calculation, this method is more than

just another model and represents the real world as well as is possible in analytic calculations at present.

While we estimate that our uncertainty is about 10% for pions, and 20% for kaons, our calculated value for the pion mass difference agrees excellently with experiment ($\Delta m_\pi^{\rm th}=4.54\pm0.50$ MeV vs $\Delta m_\pi^{\rm expt}=4.60$ MeV). In the case of kaons, our calculated value is $\Delta m_K^{\rm th}=2.6\pm0.6$ MeV, indicating a strong breaking of Dashen's theorem ($\Delta m_K^{\rm DT}=1.3$ MeV), in agreement with many other recent works [3–5].

In the next section, we briefly review the physics and history of the calculations of electromagnetic mass differences. Section III presents the basics of the Cottingham method, while Sec. IV describes our application of it to the pion mass difference. The kaon mass difference is studied in Sec. V, and we summarize our findings in Sec. VI.

II. REVIEW OF THE PROBLEM

The mass differences of kaons and pions

$$\Delta m_\pi^{\rm expt}\equiv m_{\pi^\pm}-m_{\pi^0}=4.5936\pm0.0005\ \text{MeV},$$

$$\Delta m_K^{\rm expt}\equiv m_{K^\pm}-m_{K^0}=-3.995\pm0.0034\ \text{MeV}, \tag{2}$$

or

$$\Delta m_\pi^2=2m_\pi^{(\rm avg)}\Delta m_\pi=(1.2612\pm0.0001)\times10^{-3}\ \text{GeV}^2,$$

$$\Delta m_K^2=2m_K^{(\rm avg)}\Delta m_K=(-3.9604\pm0.0035)\times10^{-3}\ \text{GeV}^2, \tag{3}$$

where $m_{K,\pi}^{(\rm avg)}\equiv 1/2[m_{(K,\pi)^\pm}+m_{(K,\pi)^0}]$ are because of two sources: quark masses and electromagnetic interactions. The difference in mass of the up and down quarks can produce isospin breaking in hadron masses. However, because the quark mass splitting is $\Delta I=1$ and the pion mass difference is only sensitive to $\Delta I=2$ effects, the pion mass difference only receives contributions of second order, i.e., $(m_d-m_u)^2$. In fact, the leading effect of this order is calculable in chiral perturbation theory:

$$\Delta m^2_{\pi({\rm QM})}=\frac{1}{4}\frac{(m_u-m_d)^2}{(m_u+m_d)(m_s-\hat m)}m^2_{\pi^\pm}, \tag{4}$$

and is quite small. To the level of our approximations we will neglect this quark mass effect and treat the pion mass difference as purely electromagnetic. The kaon mass difference, on the other hand, does receive an important contribution linear in m_d-m_u

$$\Delta m^2_{K({\rm QM})}=\frac{m_u-m_d}{m_u+m_d}m_\pi^2+O((m_u-m_d)^2). \tag{5}$$

This relation is one of the primary sources of information on quark mass ratios. For it to be useful we need to known how much of the kaon mass difference is because of electromagnetic interactions.

We have one handle on the electromagnetic mass differences which comes purely from symmetry considerations. The electromagnetic interaction explicitly violates chiral SU(3) symmetry, and its effect can be described within the chiral energy expansion. At lowest order, which is order p^0, the unique effective Lagrangian with the right symmetry-breaking properties is

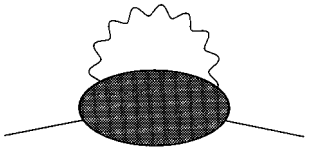

FIG. 1. Electromagnetic self-energy.

$$\mathcal{L}_0=g_{\rm EM}{\rm Tr}(QUQU^+). \tag{6}$$

This Lagrangian produces no shift in the masses of neutral mesons and equal shifts for π^+ and K^+, so that it results in

$$\Delta m_\pi^2=\Delta m_K^2. \tag{7}$$

This equality is known in the literature as Dashen's theorem [9]. It is valid in the limit of vanishing quark masses (u, d, and s) and hence of massless pions and kaons. There are a large number of effective Lagrangians possible with extra derivatives and/or factors of the quark masses, so that Dashen's theorem will receive corrections of order m_s or, equivalently, of order m_K^2 [18]. Unfortunately, the coefficients of the higher order Lagrangians are not known, so that one cannot obtain the corrections to Dashen's theorem from symmetry considerations. A direct calculation is required.

In order to obtain the electromagnetic mass shifts, one must calculate

$$\delta m^2=\frac{ie^2}{2}\int d^4x\langle\pi(p)|T[J_\mu(x)J_\nu(0)]|\pi(p)\rangle D_F^{\mu\nu}(x) \tag{8}$$

as in Fig. 1.

In momentum space this is

$$\delta m^2=\frac{ie^2}{2}\int\frac{d^4q}{(2\pi)^4}\frac{g^{\mu\nu}T_{\mu\nu}(q^2,p\cdot q)}{q^2+i\epsilon}, \tag{9}$$

where

$$T_{\mu\nu}(q^2,p\cdot q)=i\int d^4x e^{-iq\cdot x}\langle\pi(p)|T[J_\mu(x)J_\nu(0)]|\pi(p)\rangle. \tag{10}$$

This calculation is different from standard calculations within chiral perturbation theory, because we need to be able to explicitly calculate (and not just parametrize) the medium energy and high energy contributions.

There are a few things that we know rigorously about the calculation. Within QCD, the high energy renormalization of a quark mass involves a logarithmic divergence which is proportional to the quark mass itself. Therefore the pion mass difference can pick up divergences only proportional to the second power of the quark masses, which will go into defining renormalized masses in Eq. (4). In our approximation, or more strictly in the chiral limit, the pion electromagnetic mass difference is finite. For the kaon there may appear a divergence of order αm_u or αm_d, i.e., suppressed by one power of the light quark masses. This goes into a renormalization of the quark masses in Eq. (5). In principle, there is an ambiguity about how much of the electromagnetic interaction goes into the renormalized values of the quark masses. This can only be solved by a precise renormalization condi-

tion which defines the renormalized quark masses. However, because this ambiguity is proportional to αm_u and αm_d, while the kaon mass difference needs only one factor of α *or* $(m_d - m_u)$, this ambiguity is tiny and is far below the sensitivity of our calculation.

The earliest attempts at explicit calculations (Riazuddin [19] and Socolow [20]) appeared plausible but can now be recognized as mistreating the chiral portions of the calculation. The earliest valid method, and still a remarkably beautiful result, came in the work of Das *et al.* [21]. Here soft pion theorems were used to turn the matrix element of Eq. (10) into a vacuum polarization function, which in turn can be written as a dispersion relation in terms of the spectral functions of the vector and axial-vector currents, yielding the formula quoted in Eq. (1). Since QCD satisfies the chiral and high energy properties assumed in the original derivations, this remains an exact statement of QCD in the limit $m_u = m_d = 0$. The original authors saturated the spectral functions by a single vector and axial-vector pole satisfying the Weinberg sum rules [22], leading to a remarkably good value $\Delta m_\pi^{Das} = 5.0$ MeV. More recently, this sum rule has been explored using the measured spectral functions from e^+e^- annihilation and τ decay, plus QCD constraints [13]. These show that the physics of the pion mass difference is remarkably simple in the chiral limit with the most important effects being those of the lightest resonance contributions. The Das *et al.* calculation remains a benchmark for other calculations and will be an important constraint on our work.

Through the experience of the past decade of studies of chiral perturbation theory, we have gained some insight into the physics of intermediate energies. This leads to model attempts to calculate electromagnetic mass differences [5]. These calculations showed a large breaking (up to a factor of 2) of Dashen's theorem because of mass effects. To a large extent the violation of Dashen's theorem has a simple kinematic origin in the pseudoscalar propagators of the one-loop diagram.[1] Lattice simulations have also recently been started to be applied to this problem. They also see a significant violation of Dashen's theorem, $(\Delta m_K = 1.9$ MeV) [10].

III. THE COTTINGHAM METHOD AND MESON MASS SHIFT

The nonleptonic matrix element which we must calculate is given in Eq. (10). If we decompose the Compton amplitude in terms of gauge-invariant tensors, we can define

$$T_{\mu\nu}(q^2, p\cdot q) = D_{1\mu\nu} T_1(q^2, p\cdot q) + D_{2\mu\nu} T_2(q^2, p\cdot q),$$

$$D_{1\mu\nu} = -g_{\mu\nu} + \frac{q_\mu q_\nu}{q^2},$$

$$D_{2\mu\nu} = \frac{1}{p^2}\left(p_\mu - \frac{p\cdot q}{q^2} q_\mu\right)\left(p_\nu - \frac{p\cdot q}{q^2} q_\nu\right). \tag{11}$$

We have used the standard definitions for these tensors. Note that in the soft-pion limit, i.e., $p_\mu \to 0$, the combination $D_{2\mu\nu} T_2$ vanishes as we will see in the following section.

A first step consists of a rotation in the complex plane and a change of variables. We work in the pion rest frame, $p\cdot q = m_\pi q_0$. Since the singularities in $T_{\mu\nu}$ are located just below the positive real axis and above the negative real axis in the complex q_0 plane, the integration over q_0 may be rotated to the imaginary axis, $q_0 \to i q_0$, without encountering any singularities. After this transformation the integral involves only spacelike moments for photons, i.e., $q^2 \equiv -Q^2 = -(q_0^2 + \vec{q}^2)$, and the mass shift becomes

$$\delta m^2 = \frac{e^2}{2} \int \frac{d^3\vec{q}\, dq_0}{(2\pi)^4} \frac{g^{\mu\nu} T_{\mu\nu}(\vec{q}, i q_0)}{q_0^2 + \vec{q}^2}. \tag{12}$$

A change of variables from $(\vec{q}, q_0)$ to (Q^2, ν), where $\nu = m_\pi q_0$, involves

$$\int d^3\vec{q}\, dq_0 = 2\pi \int_0^\infty dQ^2 \int_{m_\pi Q}^{-m_\pi Q} \frac{d\nu}{m_\pi^2} \sqrt{m_\pi^2 Q^2 - \nu^2}, \tag{13}$$

which converts the mass shift to

$$\begin{aligned}\delta m^2 &= \frac{e^2}{16\pi^3} \int_0^\infty dQ^2 \int_{-m_\pi Q}^{m_\pi Q} \frac{d\nu}{m_\pi^2} \frac{\sqrt{m_\pi^2 Q^2 - \nu^2}}{Q^2} \\ &\quad \times g^{\mu\nu} T_{\mu\nu}(-Q^2, i\nu) \\ &= \frac{e^2}{16\pi^3} \int_0^\infty dQ^2 \int_{-m_\pi Q}^{m_\pi Q} \frac{d\nu}{m_\pi^2} \frac{\sqrt{m_\pi^2 Q^2 - \nu^2}}{Q^2} \\ &\quad + \left[-3T_1(-Q^2, i\nu) + \left(1 - \frac{\nu^2}{m_\pi^2 Q^2}\right) T_2(-Q^2, i\nu) \right].\end{aligned} \tag{14}$$

This has reduced the mass shift to an integration over the forward Compton scattering amplitude for spacelike photons.

The reduced Compton amplitudes T_1 and T_2 are presently required to be evaluated at imaginary momenta, $i\nu$. However, they can be written in terms of physical amplitudes via dispersion relations. The Compton amplitudes are known to obey dispersion relations in the ν variable with that for T_1 requiring one subtraction:

$$T_1(q^2, \nu) = T_1(q^2, 0) + \frac{\nu^2}{\pi} \int_0^\infty \frac{d\nu'^2}{\nu'^2} \frac{\mathrm{Im} T_1(q^2, \nu')}{\nu'^2 - \nu^2},$$

$$T_2(q^2, \nu) = \frac{1}{\pi} \int_0^\infty d\nu'^2 \frac{\mathrm{Im} T_2(q^2, \nu')}{\nu'^2 - \nu^2}. \tag{15}$$

The imaginary part of the forward scattering amplitudes Im T_i are defined as electron scattering structure functions

$$\frac{1}{\pi} \mathrm{Im} T_i(-Q^2, \nu) = W_i(-Q^2, \nu) \quad \text{for } i = 1,2. \tag{16}$$

After employing these dispersion relations, the integration over ν can be done explicitly with the result

[1] As was pointed out in Ref. [2], Ref. [5] has an error in one of the mass effects. The correct amplitude is shown in Eq. (25) of this paper. We disagree with the methodology of Ref. [2] which attempted to correct this problem, and agree with the critique of [2] which is contained in [4].

$$\Delta m^2=\frac{\alpha}{4\pi}\int_0^\infty\frac{dQ^2}{Q^2}\left\{-\frac{3}{2}Q^2T_1(-Q^2,0)\right.$$

$$+3Q^2\int_0^\infty\frac{d\nu'^2}{\nu'^2}W_1(-Q^2,\nu')\Lambda_1\left(\frac{\nu'^2}{m_\pi^2Q^2}\right)$$

$$\left.+\int_0^\infty\frac{d\nu'^2}{m_\pi^2}W_2(-Q^2,\nu')\Lambda_2\left(\frac{\nu'^2}{m_\pi^2Q^2}\right)\right\},\qquad(17)$$

where

$$\Lambda_1(y)\equiv\frac{1}{2}+y-y\sqrt{1+\frac{1}{y}},$$

$$\Lambda_2(y)\equiv-\frac{3}{2}-y+(1+y)\sqrt{1+\frac{1}{y}}.\qquad(18)$$

These manipulations have transformed the mass shifts into integrations over the structure functions in the physical region, as well as the subtraction term $T_1(-Q^2,0)$. The (Q^2,ν) plane is shown in Fig. 3 below, as is the physical region where $W_i\neq0$.

IV. THE PION EM MASS DIFFERENCE

In this section, we describe the details of the calculation of the electromagnetic mass difference of the pion. The exact result of the Das *et al.* [21] calculation in the chiral limit involves the difference of spectral functions $\rho_V(s)-\rho_A(s)$. This difference is entirely determined by the leading vector and axial-vector resonances. Therefore, our first step is to study the low energy chiral amplitudes supplemented by the interactions of vector and axial-vector resonances. These have been previously studied in a model field-theoretic calculation [5]. We correct the mistake found in that work [2], and transform the results into our dispersive framework. This allows us to show how the Cottingham method merges with the chiral limit result of Das *et al.* as $m_\pi\to0$.

We subsequently generalize the calculation by treating the resonances more realistically and adding in other ingredients to the amplitude. The former improvement involves the replacement of the ''narrow-width'' treatment of the resonances, which occurs in any field-theoretic treatment, by spectral functions which account for the energy variation and width of the resonances. To complete the ingredients to the calculation, we add resonance transitions not accounted for previously and also the deep inelastic continuum. The resonance couplings follow from experiment, and their presence in the Compton amplitude is confirmed by the comparison of theory and experiment in $\gamma\gamma\to\pi^0\pi^0$ [14,15,17,23]. The deep inelastic region cancels in the mass difference to the order that we are working, so that we include only a few comments on the matching of low and high energies.

Lagrangian with spin-1 resonances. Our starting point for calculating the pion Compton scattering amplitude is a Lagrangian which includes $O(E^2)$ chiral terms and $O(E^4)$ vector ($J^{PC}=1^{--}$) and axial-vector ($J^{PC}=1^{++}$) couplings, introduced by Ecker *et al.* [24,25]. This Lagrangian provides an accurate description at low and medium energies (up to ~1 GeV):

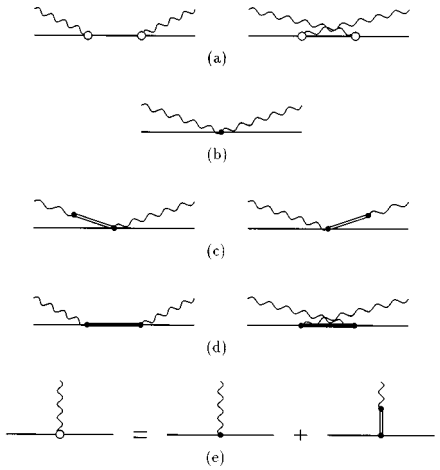

FIG. 2. Compton scattering diagrams for the meson resonances. (a) Elastic diagrams. (b) Pseudoscalar sea gull diagram. (c) Vector resonance sea gull diagrams. (d) Axial-vector resonance intermediate state diagrams. (e) Pion form factor diagrams.

$$\mathcal{L}=-\frac{1}{4}F_{\mu\nu}F^{\mu\nu}+\frac{F_\pi^2}{4}\mathrm{Tr}(D_\mu UD^\mu U^\dagger+\chi U^\dagger+\chi^\dagger U)$$

$$-\frac{1}{2}\mathrm{Tr}\left(\nabla^\lambda V_{\lambda\nu}\nabla_\nu V^{\nu\mu}-\frac{1}{2}M_V^2V^{\mu\nu}V_{\mu\nu}\right)$$

$$+\frac{F_V}{2\sqrt{2}}\mathrm{Tr}(V_{\mu\nu}f_+^{\mu\nu})+\frac{iG_V}{\sqrt{2}}\mathrm{Tr}(V_{\mu\nu}u^\mu u^\nu)$$

$$-\frac{1}{2}\mathrm{Tr}\left(\nabla^\lambda A_{\lambda\nu}\nabla_\nu A^{\nu\mu}-\frac{1}{2}M_A^2A^{\mu\nu}A_{\mu\nu}\right)$$

$$+\frac{F_A}{2\sqrt{2}}\mathrm{Tr}(A_{\mu\nu}f_-^{\mu\nu}).\qquad(19)$$

The notation is defined in the appendix. The relevant terms after expanding the above Lagrangian in terms of pion, photon, and spin-1 resonance fields are

$$\mathcal{L}=ieA^\mu(\pi^+\partial_\mu\pi^--\pi^-\partial_\mu\pi^+)+e^2A^\mu A_\mu\pi^+\pi^-$$

$$-\frac{eF_V}{2}F^{\mu\nu}\rho^0_{\mu\nu}\left(1-\frac{\pi^+\pi^-}{F_\pi^2}\right)$$

$$+\frac{iG_V}{F_\pi^2}\rho^0_{\mu\nu}(\partial^\mu\pi^+\partial^\nu\pi^-+\partial^\mu\pi^-\partial^\nu\pi^+)$$

$$-\frac{2eG_V}{F_\pi^2}A^\mu\rho^0_{\mu\nu}(\pi^+\partial^\nu\pi^-+\pi^-\partial^\nu\pi^+)$$

$$-\frac{ieF_A}{2F_\pi}F^{\mu\nu}(a_{1_{\mu\nu}}^-\pi^+-a_{1_{\mu\nu}}^+\pi^-).\qquad(20)$$

The Feynman diagrams which contribute to the pion Compton scattering amplitude, given by the above Lagrang-

ian, are shown in Fig. 2. It is convenient to classify these diagrams in three groups, which correspond with three gauge-invariant terms of the amplitude.

The first term encloses the contribution given by Figs. 2(a), and 2(b),

$$T^{(1)}_{\mu\nu}(q^2,p\cdot q)=-2D_{1_{\mu\nu}}+4m_\pi^2|G_\pi(q^2)|^2 \times\left(\frac{1}{m_\pi^2-(p+q)^2-i\epsilon} + \frac{1}{m_\pi^2-(p-q)^2-i\epsilon}\right)D_{2_{\mu\nu}}, \tag{21}$$

where we have used the vector resonance dominance approximation in the pion form factor, i.e.,

$$\frac{F_V G_V}{F_\pi^2}=1. \tag{22}$$

This is equivalent to saturating the pion form factor with the ρ meson resonance:

$$G_\pi(q^2)=\frac{m_\rho^2}{m_\rho^2-q^2}. \tag{23}$$

The second term, which we call the vector seagull, is given in Fig. 2(c). It differs from the pseudoscalar sea gull because one of the photon lines interacts through a vector resonance,

$$T^{(2)}_{\mu\nu}(q^2,p\cdot q)=-2\frac{F_V^2}{F_\pi^2}\frac{q^2}{m_\rho^2-q^2}D_{1_{\mu\nu}}. \tag{24}$$

The third group, because of the axial-vector intermediate state, given by the diagrams in Fig. 2(d), is

$$T^{(3)}_{\mu\nu}(q^2,p\cdot q)=\frac{F_A^2}{F_\pi^2 m_A^2}\left(\frac{(p\cdot q+q^2)^2+q^2[m_A^2-(p+q)^2]}{m_A^2-(p+q)^2-i\epsilon} + \frac{(p\cdot q-q^2)^2+q^2[m_A^2-(p-q)^2]}{m_A^2-(p-q)^2-i\epsilon}\right)D_{1\mu\nu} + \frac{F_A^2}{F_\pi^2 m_A^2}\left(\frac{-m_\pi^2 q^2}{m_A^2-(p+q)^2-i\epsilon} + \frac{-m_\pi^2 q^2}{m_A^2-(p-q)^2-i\epsilon}\right)D_{2\mu\nu}. \tag{25}$$

The numerical values that we use for the parameters involved in the previous five equations are

$$m_\pi=m_{\pi^\pm}=0.139\ 569\ 95\pm 0.000\ 000\ 35\ \text{GeV},$$

$$F_\pi=0.0924\pm 0.0003\ \text{GeV},$$

$$m_V=0.7699\pm 0.0008\ \text{GeV},$$

$$F_V=0.1529\pm 0.0036\ \text{GeV}. \tag{26}$$

For the numerical results in the soft-pion limit, we use the axial-vector resonance parameters, m_A, and F_A, obtained by the Weinberg sum rules [22] in the narrow-width approximation,

$$F_A^{(\mathrm{WSR})}=\sqrt{F_V^2-F_\pi^2}=0.1218\pm 0.0045\ \text{GeV},$$

$$m_A^{(\mathrm{WSR})}=\frac{F_V m_V}{F_A}=0.9664\pm 0.0427\ \text{GeV}. \tag{27}$$

The p^2 corrections to the final m_A, and F_A which we use in our final numerical answer at the end of this section, even though necessary to cancel divergences, are minimal and also have a minute effect on the numerical results for Δm_π.

Beyond the narrow-width approximation. The above analysis utilizes zero-width ρ and a_1 resonances. This ''narrow-width'' approximation is a poor description for these resonances since they are not particularly narrow, especially the a_1. The full resonance spectrum can be taken into account by employing the spectral function, Källen-Lehmann, representation [26,27]. Furthermore, this representation includes the effect of higher mass resonances with the same quantum numbers such as ρ''s in the vector case. The spectral function representation of these resonances generalizes the spin-1 resonance propagators encountered in the Compton scattering amplitudes, $T^{(i)}_{\mu\nu}(q^2,p\cdot q)$ (for $i=1-3$) given above:

$$\frac{1}{m^2-q^2-i\epsilon}\rightarrow\int ds\,\frac{\rho^R(s)}{s-q^2-i\epsilon}. \tag{28}$$

The sum of the three terms, Eqs. (21), (24), and (25), of the pion forward Compton scattering amplitude in the spectral function representation reads

$$T_{\mu\nu}(q^2,p\cdot q)=D_{1_{\mu\nu}}\left\{-2-\frac{2}{F_\pi^2}\int_0^\infty ds\rho_V^R(s)\frac{q^2}{s-q^2}+\frac{1}{F_\pi^2}\int_0^\infty ds\frac{\rho_A^R(s)}{s}\left(\frac{(p\cdot q+q^2)^2+q^2[s-(p+q)^2]}{s-(p+q)^2-i\epsilon}+(q\to -q)\right)\right\}$$
$$+D_{2_{\mu\nu}}\left\{4m_\pi^2\left|G_\pi(q^2)\right|^2\left(\frac{1}{m_\pi^2-(p+q)^2-i\epsilon}+(q\to -q)\right)\right.$$
$$\left.+\frac{1}{F_\pi^2}\int_0^\infty ds\frac{\rho_A^R(s)}{s}\left(\frac{-m_\pi^2q^2}{s-(p+q)^2-i\epsilon}+(q\to -q)\right)\right\}. \tag{29}$$

The narrow-width result can be readily reproduced by letting

$$\rho_{V,A}^{R(\mathrm{NW})}(s)=F_{V,A}^2\delta(s-m_{V,A}^2), \tag{30}$$

where the values for F_V, F_A, m_V, and m_A are given in Eqs. (26) and (27).

The Cottingham approach. Since we have a complete form for the Compton scattering amplitude we could directly calculate the pion EM mass difference with Eq. (9), avoiding the Cottingham method altogether. Nevertheless, the Cottingham method [28] allows us to gain control and insight into the calculation. This method requires the breakdown of the scattering amplitude into subtraction and structure functions terms, which are easily extracted from Eq. (29):

$$T_1(-Q^2,0)=-2+\frac{2}{F_\pi^2}\int_0^\infty ds\rho_V^R(s)\frac{Q^2}{s+Q^2}$$
$$-\frac{2}{F_\pi^2}\int_0^\infty ds\rho_A^R(s)\frac{Q^2}{s-p^2+Q^2}\left(1-\frac{p^2}{s}\right),$$

$$W_1(-Q^2,\nu)=\frac{1}{F_\pi^2}\int_0^\infty ds\frac{\rho_A^R(s)}{s}(\nu-Q^2)^2$$
$$\times\delta(s-p^2+Q^2-2\nu),$$

$$W_2(-Q^2,\nu)=4m_\pi^2\left(\frac{m_\rho^2}{m_\rho^2+Q^2}\right)^2\delta(Q^2-2\nu)$$
$$+\frac{1}{F_\pi^2}\int_0^\infty ds\frac{\rho_A^R(s)}{s}p^2Q^2\delta(s-p^2+Q^2-2\nu). \tag{31}$$

Before we describe each of these terms in detail, it is useful to be more familiar with their domain in the (ν,Q^2) plane. The subtraction term is the value of T_1 along the negative Q^2 axis. The structure functions are limited by kinematics to a sector of the first quadrant and their domain is better understood if we introduce the Bjorken scaling variable, $x=Q^2/2\nu$. The allowed kinematic ranges for the variables involved are

$$0\leqslant Q^2\leqslant\infty,\quad c\leqslant\nu\leqslant\infty,\quad \text{and } 0\leqslant x\leqslant 1,\ \text{where } c=\frac{Q^2}{2}. \tag{32}$$

The domain of both structure functions in the (ν,Q^2) plane covers the area in the first quadrant which lies between the positive ν axis ($x=0$) and the elastic line ($x=1$). This is the unshaded region shown in Fig. 3 for pion kinematics. Within this sector, the figure shows other lines of constant x which help describe the structure functions in the scaling region. It also shows two lines of constant $s=m_R^2$ which mark the region where the resonant intermediate states are the dominant contribution.

The scaling region for nucleons is the region above $Q^2\sim 1$ GeV. It is described by perturbative QCD. The relevant degrees of freedom are quarks and gluons, and the structure functions are described in terms of quark distribution functions, which depend only on x if we neglect logarithmic deviations. In this approximation, the structure functions are constant along the constant-x lines.

The resonance region in the (ν,Q^2) plane is described by the two dashed lines parallel to the elastic or $x=1$ line. These lines satisfy the equation for constant squared invariant mass of intermediate resonant states:

$$M_R^2=(p+q)^2=p^2+2\nu-Q^2. \tag{33}$$

Since the graph is for pion values we choose the a_1 as the first resonance, $m_{a_1}=1.26$ GeV. We also include a second resonance with mass $m_R=\sqrt{2}m_{a_1}$ in order to show the position of possible higher resonances.

This resonance region is described by chiral Lagrangians which include spin-1 resonances such as Eq. (19) [24,25]. The structure functions obtained through the chiral

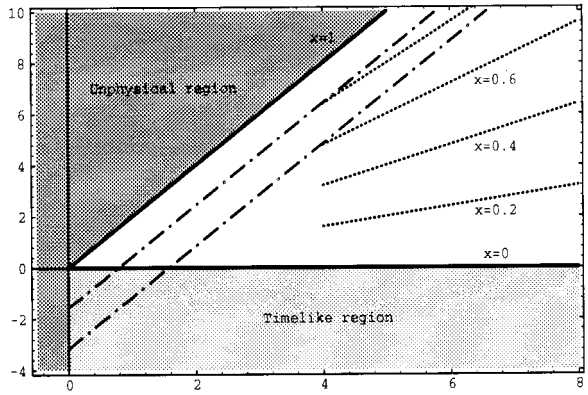

FIG. 3. (ν,Q^2) plane. Units in GeV^2. Unshaded region is the domain of the structure functions. Dashed and solid lines are for $x=$ 0, 0.2, 0.4, 0.6, 0.8, and 1.0. Dashed-dotted lines are for $M_R^2=$ 1.6 and 3.2 GeV^2.

Lagrangians in the narrow-width approximation are constrained to the elastic line, the a_1 line, plus other parallel lines corresponding to possible higher resonances. If we include a finite width for the resonances, these lines become bands whose thickness is proportional to the resonance width.

The usefulness of applying the Cottingham method arises from the breakdown of the scattering amplitude into the three terms shown in Eq. (31). We gain control because we can make reasonable assumptions and establish constraints on the pion structure functions. At the same time, it is possible to relate the subtraction term to the soft-pion limit.

All of the resonance couplings will contain form factors which suppress the effect of an individual resonance as $Q^2 \to \infty$. We will assume that the fall off of all such photon form factors will involve a scale which is a typical vector-meson mass. We now turn to the procedure to introduce these form factors in our dispersive framework. This has a subtlety in that some naive structures for this form factor could upset the soft-pion limits in our formulas. We will choose a form which is well behaved in the soft-pion limit. The form factor also solves what would appear to be a problem in the present inclusion of resonances, i.e., the structure function $W_1(Q^2,\nu)$ given in Eq. (31) has terms proportional to ν^2 and Q^4 which would generate divergences for large Q^2. This does not occur in the presence of the form factors. This divergent behavior is clear if we calculate $W_1(Q^2,\nu)$ along the lines of constant $s=m_R^2$. We use the δ function to eliminate the ν dependence, i.e., $\nu=\frac{1}{2}(s-p^2+Q^2)$, to obtain

$$W_1^{(cst.\ s)}(Q^2,\nu)=\frac{1}{F_\pi^2}\frac{\rho_A^R(s)}{s}\frac{1}{4}(s-p^2-Q^2)^2, \qquad (34)$$

which diverges as Q^4. A structure function for a given resonant state cannot diverge for large Q^2 without violating unitarity. For a single resonance, as it is the case in question, the structure function must go to zero if we follow a line of constant invariant mass s to high energies. In order to achieve this behavior, we introduce a multiplicative factor which forces its convergence. This factor $K(\nu,s)$ resembles the form factor obtained for the elastic term through the vector-meson dominance model. In addition, it has the properties

$$K(\nu=0,s)=1,$$

$$\lim_{Q^2\to\infty} K(\nu,s)^{(cst.\ s)} \sim \frac{1}{Q^6},$$

$$[K(\nu,s)^{(cst.\ s)}]_{Q^2=0}=1. \qquad (35)$$

These properties ensure that the subtraction term is left unchanged, and that the structure function will converge for large Q^2. The form factor is normalized in order to agree with the previous result at $Q^2=0$ for fixed s. The form factor that satisfies these conditions is

$$K(\nu,s)=\left(\frac{m_V^2}{m_V^2+2\nu}\right)^4\left(1+\eta\frac{2\nu}{s}\right), \qquad (36)$$

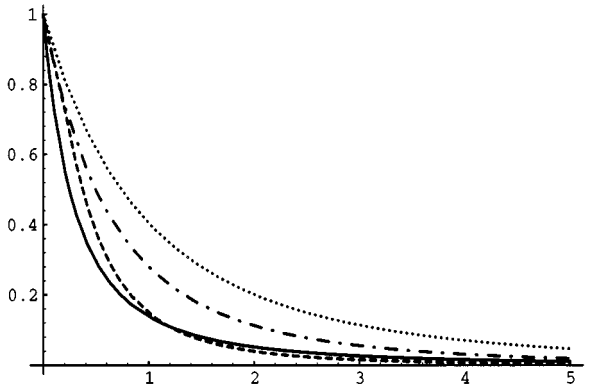

FIG. 4. Factor $K(\nu,s)$ and pion EM form factor vs Q^2. Pion EM form factor, solid line. $K(\nu,m_\pi^2)$, dashed line. $K(\nu,1\ \mathrm{GeV}^2)$, dash-dotted line. $K(\nu,2\ \mathrm{GeV}^2)$, dotted line. Horizontal scale represents Q^2 in GeV^2.

where

$$\eta=\frac{s}{s-p^2}\left[\left(1+\frac{s-p^2}{m_V^2}\right)^4-1\right], \qquad (37)$$

and $p^2=m_\pi^2$. We have chosen the appropriate value for the vector-meson mass, $m_V=m_\rho$. The factor $K(\nu,s)$ above also has the property of being very close to the ρ contribution to the pion EM form factor for $s=p^2$, as it can be seen in Fig. 4.

The inclusion of this factor in our analysis is easily achieved through the substitution

$$\rho_A^R(s)\to\rho_A^R(s)K(\nu,s). \qquad (38)$$

The structure functions and subtraction terms read

$$T_1(-Q^2,0)=-2+\frac{2}{F_\pi^2}\int_0^\infty ds\,\rho_V^R(s)\frac{Q^2}{s+Q^2} - \frac{2}{F_\pi^2}\int_0^\infty ds\,\rho_A^R(s)\frac{Q^2}{s-p^2+Q^2}\left(1-\frac{p^2}{s}\right),$$

$$W_1(-Q^2,\nu)=\frac{1}{F_\pi^2}\int_0^\infty ds\,\frac{\rho_A^R(s)}{s}K(\nu,s)(\nu-Q^2)^2 \times\delta(s-p^2+Q^2-2\nu), \qquad (39)$$

$$W_2(-Q^2,\nu)=4m_\pi^2\left(\frac{m_\rho^2}{m_\rho^2+Q^2}\right)^2\delta(Q^2-2\nu) + \frac{1}{F_\pi^2}\int_0^\infty ds\,\frac{\rho_A^R(s)}{s}K(\nu,s) \times p^2Q^2\delta(s-p^2+Q^2-2\nu).$$

The pion EM mass difference for the above functions is readily obtained with Eq. (17). We choose to break it into terms corresponding to those shown in the above equation with an extra subdivision of the W_2 contribution which isolates the elastic term

$$\Delta m_\pi^2(\text{subtr}) = \frac{\alpha}{4\pi}\int_0^\infty dQ^2 \frac{3}{F_\pi^2}\left[F_\pi^2 - \int_0^\infty ds \rho_V^R(s) \frac{Q^2}{s+Q^2} + \int_0^\infty ds \rho_A^R(s) \frac{Q^2}{s-p^2+Q^2}\left(1-\frac{p^2}{s}\right)\right],$$

$$\Delta m_\pi^2(W_1) = \frac{\alpha}{4\pi}\int_0^\infty dQ^2 \frac{6}{F_\pi^2}\int_0^\infty ds \frac{\rho_A^R(s)}{s}\frac{1}{\Delta^2}\left(\frac{\Delta^2}{2}-Q^2\right)^2 \times \Lambda_1\left(\frac{\Delta^4}{4p^2Q^2}\right) K\left(\frac{\Delta^2}{2},s\right),$$

$$\Delta m_\pi^2(\text{elast}) = \frac{\alpha}{4\pi}\int_0^\infty dQ^2 \left(\frac{m_\rho^2}{m_\rho^2+Q^2}\right)^2 \Lambda_2\left(\frac{Q^2}{4p^2}\right),$$

$$\Delta m_\pi^2(W_2) = \frac{\alpha}{4\pi}\int_0^\infty dQ^2 \frac{1}{2F_\pi^2}\int_0^\infty ds \frac{\rho_A^R(s)}{s} \times \Delta^2 \Lambda_2\left(\frac{\Delta^4}{4p^2Q^2}\right) K\left(\frac{\Delta^2}{2},s\right), \tag{40}$$

where $\Delta^2 = s - p^2 + Q^2$, and $\Lambda_i(y)$ (for $i=1,2$) are defined in Eq. (18).

High energy constraints. Even though we can obtain an explicit formula for the pion EM mass difference by adding all the contributions in Eqs. (40), it is necessary to analyze the upper limit of the Q^2 integral. Adding all the different contributions in Eqs. (40), and expanding the Q^2 integrand in powers of $1/Q^{2n}$, we obtain

$$-\left(\frac{3\alpha}{4\pi F_\pi^2}\right)\left\{ -F_\pi^2 + \int_0^\infty ds\left[\rho_V^R(s) - \rho_A^R(s)\left(1-\frac{p^2}{s}\right)\right]\right\}\frac{1}{Q^0} + \left(\frac{3\alpha}{4\pi F_\pi^2}\right)\int_0^\infty ds s\left[\rho_V^R(s) - \rho_A^R(s)\left(1-\frac{p^2}{s}\right)^2\right]\frac{1}{Q^2} + O\left(\frac{1}{Q^4}\right), \tag{41}$$

where, $p^2 = m_\pi^2$. If the first two terms are not zero, they originate linear and logarithmic divergences, respectively. In order to obtain a finite pion EM mass difference we cancel them explicitly generating two constraint equations,

$$\int_0^\infty ds\left[\rho_V^R(s) - \rho_A^R(s)\left(1-\frac{p^2}{s}\right)\right] = F_\pi^2, \tag{42}$$

$$\int_0^\infty ds s\left[\rho_V^R(s) - \rho_A^R(s)\left(1-2\frac{p^2}{s}+\frac{p^4}{s^2}\right)\right] = 0. \tag{43}$$

These high Q^2 constraints become the Weinberg sum rules in the soft-pion limit, which in the above equations is obtained by letting $p^2 = 0$. We will see later a more detailed explanation of this limit and its relation to the subtraction term.

Because of the introduction of the convergence factor $K(\nu,s)$, the above divergences originate only from the subtraction term. We incorporate the high Q^2 constraints in the subtraction term of the pion EM mass difference, Eq. (40), in order to make all the contributions finite. The following procedure removes both divergences.

Subtract the linear divergence from the subtraction term by means of Eq. (42):

$$\begin{aligned}\Delta m_\pi^2(\text{subtr}) = \frac{\alpha}{4\pi}\int_0^\infty dQ^2 \frac{3}{F_\pi^2}\Bigg\{ & F_\pi^2 - \int_0^\infty ds \rho_V^R(s)\frac{Q^2}{s+Q^2} + \int_0^\infty ds \rho_A^R(s)\frac{Q^2}{s-p^2+Q^2}\left(1-\frac{p^2}{s}\right) \\ & - \Bigg[F_\pi^2 - \int_0^\infty ds \rho_V^R(s) + \int_0^\infty ds \rho_A^R(s)\left(1-\frac{p^2}{s}\right)\Bigg]\Bigg\} \\ = \frac{\alpha}{4\pi}\int_0^\infty dQ^2 \frac{3}{F_\pi^2}\Bigg\{ & \int_0^\infty ds \rho_V^R(s)\frac{s}{s+Q^2} - \int_0^\infty ds \rho_A^R(s)\frac{s-p^2}{s-p^2+Q^2}\left(1-\frac{p^2}{s}\right)\Bigg\}. \end{aligned} \tag{44}$$

Integrate over Q^2 and cancel the corresponding logarithmic divergence by subtracting Eq. (43) multiplied by $\ln\Lambda_{Q^2}$:

$$\begin{aligned}\Delta m_\pi^2(\text{subtr}) = \lim_{\Lambda_{Q^2}\to\infty} \frac{\alpha}{4\pi}\frac{3}{F_\pi^2}\Bigg\{ & \int_0^\infty ds s \rho_V^R(s)\ln\frac{\Lambda_{Q^2}+s}{s} - \int_0^\infty ds \rho_A^R(s)(s-p^2)\left(1-\frac{p^2}{s}\right) \\ & \times \ln\frac{\Lambda_{Q^2}+s-p^2}{s-p^2} - \Bigg[\int_0^\infty ds s \rho_V^R(s)\ln\Lambda_{Q^2} \\ & - \int_0^\infty ds \rho_A^R(s)\frac{(s-p^2)^2}{s}\ln\Lambda_{Q^2}\Bigg]\Bigg\}. \end{aligned} \tag{45}$$

Add the terms and take the limit $\Lambda_{Q^2}\to\infty$, to obtain

$$\Delta m_\pi^2(\text{subtr}) = -\frac{\alpha}{4\pi}\frac{3}{F_\pi^2}\int_0^\infty ds\Bigg[s\,\ln s\rho_V^R(s) - (s-p^2) \times \ln(s-p^2)\rho_A^R(s)\left(1-\frac{p^2}{s}\right)\Bigg]. \tag{46}$$

The above contribution is free of divergences. Furthermore, in the soft-pion limit, i.e., $p^2 = 0$, it is equivalent to the Das

et al. calculation [21]. Finally, we have a useful formula to calculate $\delta m_\pi^{(\mathrm{EM})}$ free of divergences, which was mainly the product of the Lagrangian introducing the chiral couplings of the spin-1 resonances. We proceed to show the close relation of the subtraction term and the soft-pion limit and to see how we reproduce the results of $O(p^4)$ chiral perturbation theory with the above scattering amplitude.

Soft-pion limit and its relation to the subtraction term. In the following we will show that the subtraction term is given by the soft-pion limit up to corrections of order p^2. In this discussion we refer to noncontact contributions as all contributions except the pion sea gull term. This term is the only one which has both photons interacting at the same vertex and, therefore, we treat it differently in the following discussion.

The noncontact contributions to the Compton scattering amplitude have the form

$$T_{\mu\nu}^{(\mathrm{NC})}(q^2,p\cdot q)=i\int dx e^{-iqx}\langle\pi|T[V_\mu(x)V_\nu(0)]|\pi\rangle. \tag{47}$$

Consider the soft-pion theorem [29]

$$\lim_{p_\mu\to 0}\langle\pi^k(p)\beta|O|\alpha\rangle=-\frac{i}{F_\pi}\langle\beta|[Q_5^k,O]|\alpha\rangle, \tag{48}$$

where β and α are arbitrary states and $Q_5^k=\int d^3x A_0^k(x)$ is an axial charge. We also need the commutators

$$[Q_5^i,V_\mu^j]=if^{ijk}V_\mu^k,\quad [Q_5^i,A_\mu^j]=if^{ijk}A_\mu^k. \tag{49}$$

The result of applying the soft-pion theorem to Eq. (47) is

$$\lim_{p_\mu\to 0}T_{\mu\nu}^{(\mathrm{NC})}(q^2,p\cdot q)=-i\int d^4x e^{iqx}\frac{-2}{F_\pi^2}\times\langle 0|T[V_3^\mu(x)V_3^\nu(0)-A_3^\mu(x)A_3^\nu(0)]|0\rangle. \tag{50}$$

The two-current time-ordered products are related to the spectral functions by

$$\langle 0|T[V_a^\mu(x)V_b^\nu(0)]|0\rangle=i\delta_{ab}\int_0^\infty ds\rho_V(s)(\Box g_{\mu\nu}-\partial^\mu\partial^\nu)\times\int\frac{d^4k}{(2\pi)^4}\frac{e^{-ikx}}{k^2-s+i\epsilon},$$

$$\langle 0|T[A_a^\mu(x)A_b^\nu(0)]|0\rangle=-i\delta_{ab}F_\pi^2\partial^\mu\partial^\nu\int\frac{d^4k}{(2\pi)^4}\frac{e^{-ikx}}{k^2+i\epsilon}+i\delta_{ab}\int_0^\infty ds\rho_A(s)(\Box g_{\mu\nu}-\partial^\mu\partial^\nu)\times\int\frac{d^4k}{(2\pi)^4}\frac{e^{-ikx}}{k^2-s+i\epsilon}. \tag{51}$$

Upon combining Eqs. (50) and (51), integrating over d^4x, and using the resulting δ function to integrate over d^4k, we obtain

$$\lim_{p_\mu\to 0}T_{\mu\nu}^{(\mathrm{NC})}(q^2,p\cdot q)=-2\frac{q^\mu q^\nu}{q^2+i\epsilon}+\frac{2}{F_\pi^2}\int_0^\infty ds\times\left(-g^{\mu\nu}+\frac{q^\mu q^\nu}{q^2}\right)[\rho_V(s)-\rho_A(s)]\times\frac{q^2}{q^2-s+i\epsilon}. \tag{52}$$

The contact term or pion sea gull contribution to the pion Compton scattering amplitude is

$$T_{\mu\nu}^{(\mathrm{C})}(q^2,p\cdot q)=2g_{\mu\nu}, \tag{53}$$

which remains unchanged in the soft-pion limit. Adding both contributions to the pion Compton scattering amplitude in the soft-pion limit, we obtain

$$\lim_{p_\mu\to 0}T_{\mu\nu}(q^2,p\cdot q)=D_{1_{\mu\nu}}\left\{-2+\frac{2}{F_\pi^2}\int_0^\infty ds[\rho_V(s)-\rho_A(s)]\frac{q^2}{q^2-s}\right\}. \tag{54}$$

An alternative way of reproducing the soft-pion limit result above is letting $p_\mu\to 0$ in Eq. (29). In order to implement this limit the following relations are useful:

$$\lim_{p_\mu\to 0}D_{1_{\mu\nu}}=D_{1_{\mu\nu}},$$

$$\lim_{p_\mu\to 0}p^2D_{2_{\mu\nu}}=0,$$

$$\lim_{p_\mu\to 0}T_1(q^2,p\cdot q)=T_1(q^2,0)|_{p^2=0}. \tag{55}$$

From these relations it follows that the only surviving term in this limit is the subtraction term $T_1(q^2,0)$:

$$\lim_{p_\mu\to 0}T_{\mu\nu}(q^2,p\cdot q)=D_{1_{\mu\nu}}\lim_{p_\mu\to 0}T_1(q^2,0). \tag{56}$$

This gives the same result as Eq. (54) when we identify

$$\lim_{p_\mu\to 0}(\rho_V^R(s)-\rho_A^R(s))=[\rho_V(s)-\rho_A(s)]. \tag{57}$$

We can now calculate the soft-pion limit to the pion EM mass difference:

$$\lim_{p_\mu\to 0}\Delta m_\pi^2=\frac{\alpha}{4\pi}\int_0^\infty dQ^2\frac{3}{F_\pi^2}\times\left\{F_\pi^2-\int_0^\infty ds[\rho_V(s)-\rho_A(s)]\frac{Q^2}{Q^2+s}\right\}, \tag{58}$$

where $Q^2=-q^2$. We follow the procedure described earlier in order to cancel the linear and logarithmic divergences occurring in the above equation. The cancellation of these divergences imposed by the finiteness of the pion EM mass difference requires

$$\int_0^\infty ds[\rho_V(s)-\rho_A(s)]=F_\pi^2, \tag{59}$$

$$\int_0^\infty ds s[\rho_V(s)-\rho_A(s)]=0. \tag{60}$$

These are Weinberg sum rules [22], obtained in our case as a consequence of the finiteness of $\delta m_\pi^{(\mathrm{EM})}$ in the soft-pion limit. Subtracting the linear and logarithmic divergences in the same way as for the subtraction term, Eqs. (44)–(46), we obtain

$$\lim_{p_\mu\to 0}\Delta m_\pi^2=-\frac{\alpha}{4\pi}\frac{3}{F_\pi^2}\int_0^\infty ds s\ln s[\rho_V(s)-\rho_A(s)]. \tag{61}$$

This is the result obtained by Das *et al.* [21].

Finally, we evaluate Eq. (61) in the narrow-width approximation to obtain the numerical result

$$\lim_{p_\mu\to 0}\Delta m_\pi^{(\mathrm{NW})}=4.685\ \mathrm{MeV}. \tag{62}$$

Spectral functions. We seek an improved description of the physics of the resonance region with the spectral functions $\rho_V^R(s)$ and $\rho_A^R(s)$ replacing the narrow-width description. The ingredients to the spectral functions clearly are the same resonance states that are revealed by the usual vector and axial-vector spectral functions $\rho_V(s)$ and $\rho_A(s)$. In addition, we have just seen that in the soft-pion limit there is an exact correspondence $\rho_V^R(s)-\rho_A^R(s)=\rho_V(s)-\rho_A(s)$. This leads us to utilize the experimental spectral functions determined in Ref. [13] in order to produce a shape for $\rho_V^R(s)$ and $\rho_A^R(s)$. In both the soft-pion limit and the full Cottingham calculation at order m_π^2, the high energy continuum cancels in the mass shift. We, therefore, separate each spectral function into two contributions, one because of the resonances and the other because of the high energy continuum common to both vector and axial-vector channels. The resonant part is chosen to match the resonances revealed in the phenomenological analysis of the data in [13]. These spectral functions are then slightly altered to obey the full constraint equations including p^2 terms of Eqs. (85) and (86) below. A continuum contribution, common to both vector and axial-vector channels, was included in [13], but is here kept separate from the resonances. The result of this is that we identify

$$\rho_{V,A}(s)=\rho_{V,A}^R(s)+\rho_{V,A}^C(s), \tag{63}$$

with a continuum contribution

$$\rho^C(s)=\rho_V^C(s)=\rho_A^C(s). \tag{64}$$

The precise identification of the continuum is not unique, but since the difference of spectral functions enters, reasonable variations do not produce a large final effect. The specific form that we use is shown in Fig. 5.

It is clear that the greatest source of model dependence in our calculation comes form the numerical identification described above. Our procedure in setting up the calculation in the Cottingham method is very general. However, we do not have directly available the experimental structure functions for photons scattering off of pions. We have used an identification which is valid in the chiral limit in order to provide this numerical input. There could be shifts in the couplings of these resonances which are of order m_π^2. These could provide changes in the final answer at order m_π^2 which would be of interest to us. This is partially relieved by the fact that the analysis of [13] was carried out with real world data, not strictly in the chiral limit. Thus the masses, widths, and shapes of the resonances will accurately reflect physics with $m_\pi^2\neq 0$. Likewise, we know that in the narrow-width approximation we have the right description, so that we do not see a source of major uncertainty because of the nonzero widths. This means that our model dependence comes from possible m_π^2 dependences in the resonance couplings, and our implicit assumption is that these are smaller than the m_π^2 dependence from the propagators. We have not been able to find a way to do better than this in the phenomenological analysis.

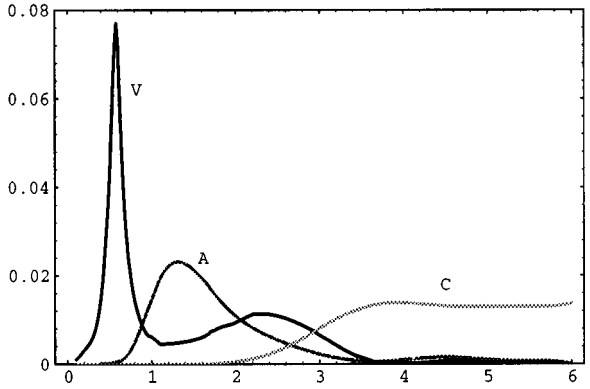

FIG. 5. Vector and axial-vector spectral functions. The graph shows (V) $\rho_V^R(s)$, (A) $\rho_A^R(s)$, and (C) $\rho_C(s)$ vs s. The s scale is given in GeV^2.

Comparison $O(E^4)$ chiral perturbation theory. We also like to compare our method to the standard chiral perturbation approach. The lowest energy region of the pion structure function can be described by the chiral SU(3) Lagrangian to order p^4, originally developed by Gasser and Leutwyler [11,12]. In addition to elastic and sea gull terms, and ignoring pion loops, the only relevant terms involved in the pion Compton scattering amplitude are the L_9 and L_{10} terms:

$$\mathcal{L}_4=-iL_9\mathrm{Tr}(F_R^{\mu\nu}D_\mu UD_\nu U^\dagger+F_L^{\mu\nu}D_\mu U^\dagger D_\nu U)+L_{10}\mathrm{Tr}(U^\dagger F_R^{\mu\nu}UF_{L\mu\nu})+\text{ other.} \tag{65}$$

The pion forward Compton scattering amplitude resulting from this Lagrangian was calculated by Bijnens and Cornet [14], and Donoghue *et al.* [15]. Their result, up to pion loop contributions which are small, is

$$T_{\mu\nu}(p,q)=-\frac{8p^2q^2}{q^4-(2p\cdot q)^2}\left(1+\frac{2L_9^r q^2}{F_\pi^2}\right)^2 D_{2_{\mu\nu}}-2D_{1_{\mu\nu}}+\frac{8L_{10}^r q^2}{F_\pi^2}D_{1_{\mu\nu}}+\text{ loops.} \tag{66}$$

Expanding our narrow-width result in powers of external momenta p_μ and q_μ, we obtain

$$T_{\mu\nu}^{(q^2\text{exp})}(q^2,p\cdot q)=D_{1_{\mu\nu}}\left\{-2-2\frac{F_V^2}{F_\pi^2}\frac{q^2}{m_\rho^2}+2\frac{F_A^2}{F_\pi^2}\frac{q^2}{m_A^2}\right\}$$
$$+D_{2_{\mu\nu}}\left\{4m_\pi^2\left(1+\frac{q^2}{m_V^2}\right)^2\frac{-2q^2}{q^4-(2p\cdot q)^2}\right.$$
$$\left.+2\frac{F_A^2}{F_\pi^2 m_A^2}\frac{-m_\pi^2 q^2}{m_A^2}\right\}$$
$$+\text{ higher order terms in }(q^2,p\cdot q,p^2). \tag{67}$$

The relations for the L_9 and L_{10} in terms of the spin-1 resonance parameters are obtained by inspection from Eqs. (66) and (67).

$$L_9=\frac{F_\pi^2}{2m_V^2},$$

$$L_{10}=-\frac{1}{4}\left(\frac{F_V^2}{m_V^2}-\frac{F_A^2}{2m_A^2}\right). \tag{68}$$

This result is in agreement with Ecker *et al.* [24]. The above equation for L_{10} is also the narrow-width approximation for the sum rule (W0) in Ref. [13].

Substituting the narrow-width parameters in Eq. (68), we obtain

$$L_9=(7.20\pm0.05)\times10^{-3},$$

$$L_{10}=-(5.89\pm0.65)\times10^{-3}. \tag{69}$$

These are seen to be within reasonable agreement with the experimental values;

$$L_9=(7.1\pm0.3)\times10^{-3},$$

$$L_{10}=-(6.84\pm0.3)\times10^{-3}. \tag{70}$$

The difference between the values in Eqs. (69) and (70) gives an estimate for the loop contributions which we neglected in the $O(p^4)$ chiral Lagrangian calculation of the Compton scattering amplitude. Besides the loop corrections, the difference can also be because of the inaccuracy of the narrow-width approximation.

Scaling region. The low and intermediate energy regions of the structure functions are described above. To complete the analysis of the structure functions we need to describe the scaling region at large values of (ν,Q^2). The ingredients and general behavior in this region are well known. The structure functions become largely functions of the Bjorken scaling variable $x=Q^2/2\nu$, with logarithmic Q^2 variations predictable by QCD [30]. This is easy to build into the Cottingham analysis [31]. However, there is not a need to describe the details here since the scaling region cancels in the difference between the charged and neutral pions masses, to the order that we are working here.

In the limit that the u and d quark masses are equal, the deep inelastic structure functions of the neutral and charged pions are equal. This leads to

$$\Delta m_\pi(\text{scaling})=0. \tag{71}$$

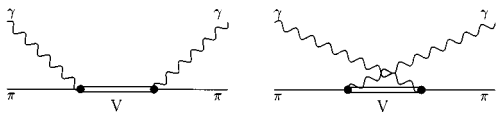

FIG. 6. Intermediate vector diagrams.

To the extent that the u, d masses are different, the structure functions may differ. However, we are calculating the electromagnetic effect in the limit $m_u=m_d$ so that we are not sensitive to this effect.

$V\to\pi\gamma$ contribution. To have a more complete phenomenological description of the Compton scattering amplitude we also include the effect of intermediate vector-meson diagrams shown in Fig. 6. The motivation for introducing these diagrams is the experimental observation of the radiative meson decays $\omega\to\pi\gamma$ and $\rho\to\pi\gamma$, and $\phi\to\pi\gamma$. The effective Lagrangian which includes the $V\pi\gamma$ vertices is

$$\mathcal{L}=e\frac{\sqrt{R_V}}{2}\epsilon^{\mu\nu\alpha\beta}F_{\mu\nu}V_\alpha\partial_\beta\pi. \tag{72}$$

This Lagrangian is invariant under parity and charge conjugation transformations, as well as under chiral rotations. The choice of including the EM field strength tensor ensures gauge invariance, and the pion momentum dependence corresponds to the correct soft-pion limit for the vertex.

We introduce the spectral functions $g_V(s)$ to describe the intermediate states in Fig. 6. The normalization of these functions is chosen in order to make the subtraction term contribution compatible with the ones obtained for the axial-vector case. The narrow-width approximation for $g_V(s)$ is

$$g_V(s)=H_V^2\delta(s-m_V^2)=F_\pi^2R_V\delta(s-m_V^2). \tag{73}$$

The subtraction term and the structure functions for the intermediate vector-meson diagrams follow from the Lagrangian in Eq. (72):

$$T_1(-Q^2,0)=\frac{2}{F_\pi^2}\int_0^\infty ds g_V(s)\frac{p^2Q^2}{s-p^2+Q^2},$$

$$W_1(-Q^2,\nu)=\frac{1}{F_\pi^2}\int_0^\infty ds g_V(s)K(\nu,s)(\nu^2+p^2Q^2)$$
$$\times\delta(s-p^2+Q^2-2\nu),$$

$$W_2(-Q^2,\nu)=\frac{1}{F_\pi^2}\int_0^\infty ds g_V(s)K(\nu,s)$$
$$\times p^2Q^2\delta(s-p^2+Q^2-2\nu), \tag{74}$$

where $K(\nu,s)$ is the factor defined in Eq. (36). The factor $K(\nu,s)$ ensures the Q^2 convergence of the structure functions as in the intermediate axial-vector state case. We only need to find the spectral function $g_V(s)$ in order to determine the above functions.

There are four possible vector intermediate states for the pion Compton amplitude, the $\rho^\pm$ for the charged pions, and the ρ^0, ω, and ϕ for the neutral pion. The coupling constants, $R_{\rho^\pm}$, R_{ρ^0}, R_ω, and R_ϕ, can be extracted from the radiative decays of these vector mesons. We refer the reader

to Refs. [17,23,32,33] for a review and examples of obtaining such couplings. The couplings $R_{\rho^\pm}$ and R_{ρ^0} are the same if we take isospin to be an exact symmetry. This means that the charged and neutral pion EM self-energies because of the ρ intermediate state would cancel in the pion EM mass difference. However, the ω and ϕ intermediate state contributions do not present such a cancellation. Since isospin-breaking effects are generally of small magnitude, we shall neglect the intermediate ρ contribution to the pion EM mass difference.

We can determine the ω coupling R_ω from the experimental measurement of the radiative decay $\omega\to\pi^0\gamma$:

$$R_\omega=\frac{24}{\alpha}\frac{m_\omega^3}{(m_\omega^2-m_\pi^2)^3}\Gamma_{\omega\to\pi\gamma}=5.40\pm0.32\ \mathrm{GeV}^{-2}. \quad (75)$$

Likewise, we determine the ϕ coupling R_ϕ:

$$R_\phi=\frac{24}{\alpha}\frac{m_\phi^3}{(m_\phi^2-m_\pi^2)^3}\Gamma_{\phi\to\pi\gamma}=0.019\pm0.002\ \mathrm{GeV}^{-2}, \quad (76)$$

where we have used the experimental values listed by the Particle Data Group [34]. We do not consider the ϕ-vector-meson intermediate state further because its coupling is an order of magnitude smaller than the experimental uncertainty of the ω coupling.

We are now ready to determine the spectral function $g_V(s)$. Since the only resonance involved is the ω, we can safely use the narrow-width approximation of Eq. (73). The width of the ω is only 1% of its mass. This is in contrast with the ρ and a_1 resonances for which the widths are 20% and 33% of their mass, respectively. In the narrow-width approximation we only need m_ω taken from [34], and H_V given by

$$H_V=F_\pi\sqrt{R_V}=0.215\pm0.013. \quad (77)$$

We should be careful when comparing $g_V(s)$ to $\rho_{V,A}(s)$ since they have different units. The relationship among these structure functions will become clear in the following subsection.

The intermediate vector meson subtraction term and structure function contributions to the pion EM mass difference are obtained by combining Eqs. (17) and (74),

$$\Delta m_\pi^2(\mathrm{subtr})=\frac{3\alpha}{4\pi F_\pi^2}\int_0^\infty dQ^2\int_0^\infty ds g_V(s)\frac{p^2Q^2}{s-p^2+Q^2}, \quad (78)$$

$$\Delta m_\pi^2(W_1)=\frac{-\alpha}{4\pi}\int_0^\infty dQ^2\frac{6}{F_\pi^2}\int_0^\infty ds g_V(s)K\left(\frac{\Delta^2}{2},s\right)\times\frac{1}{\Delta^2}\left(\frac{\Delta^4}{4}+p^2Q^2\right)\Lambda_1\left(\frac{\Delta^4}{4p^2Q^2}\right),$$

$$\Delta m_\pi^2(W_2)=\frac{-\alpha}{4\pi}\int_0^\infty dQ^2\frac{1}{2F_\pi^2}\int_0^\infty ds g_V(s)K\left(\frac{\Delta^2}{2},s\right)\times\Delta^2\Lambda_2\left(\frac{\Delta^4}{4p^2Q^2}\right),$$

where $\Delta^2=s-p^2+Q^2$, $p^2=m_\pi^2$, and the functions $\Lambda_i(y)$ for $i=1,2$ are defined in Eq. (18). The extra minus sign appears because the vector intermediate state diagrams contribute to the neutral pion EM self-energy.

General treatment of other possible contributions. At this point we have a fairly complete calculation of the pion EM mass difference broken down into different contributions. We have included the spin-1 resonances through their lowest order chiral couplings, the scaling, and the intermediate vector resonance contributions to the pion EM mass difference. By analogy with the nucleon structure functions, we are comfortable with our estimates of the structure function contributions. These are small, and even a factor of 2 correction would amount to a small correction to the total mass difference. Therefore, we concentrate in the subtraction term contribution estimate.

The subtraction term has been obtained by calculating the pion Compton scattering amplitude with the effective chiral Lagrangian for the vector and axial-vector resonances of Eq. (19) and the effective Lagrangian for the intermediate vector-meson contribution of Eq. (72). In general, there could be other possible contributions to the subtraction term. These could be introduced by higher order effective Lagrangians. Their contributions to $\delta m_\pi^{\mathrm{EM}}$ would be small since they would be of higher order in the external momenta p^2 and q^2. The terms with higher powers of p^2 are naturally small, otherwise terms of higher order in q^2 are in principle divergent. The finiteness of $\delta m_\pi^{\mathrm{EM}}$ requires that all the higher powers of q^2 cancel in the same way that the order one and $1/Q^2$ cancel because of the Weinberg sum rules in the soft-pion limit case.

We include all other possible contributions to the subtraction term, not yet accounted for in the previous analysis, by introducing the remainder term

$$\frac{2}{F_\pi^2}\int_0^\infty ds R(Q^2,p^2,s). \quad (79)$$

The purpose of including this term is to show explicitly the effect of possible corrections to our current scattering amplitude and its role in the high energy constraints and final formula for the EM mass difference.

There are some conditions required upon this remainder term. It cannot alter our previous soft-pion limit result; therefore,

$$\lim_{p_\mu\to0}\int_0^\infty ds R(Q^2,p^2,s)=0. \quad (80)$$

It is also convenient to use the following notation for its expansion in powers of $1/Q^2$:

$$R(Q^2,p^2,s)=p^2h_1(p^2,s)+\frac{p^2h_2(p^2,s)}{Q^2+f(p^2,s)}+O\left(\frac{1}{Q^4}\right). \quad (81)$$

We have explicitly introduced a factor of p^2 in order to make sure that this term vanishes in the soft-pion limit as given in Eq. (80). This limit also requires that the functions $h_i(p^2,s)$ (for $i=1,2$) do not have a pole at $p^2=0$. The above equation is not a formal expansion in orders of $1/Q^2$ since

we have introduced the function $f(p^2,s)$ in the denominator of the second term. This has been done in order to make the Q^2 integral of this term convergent at low Q^2. The reason for choosing the above notation will be clear in the following extraction of the subtraction term contribution to $\delta m_\pi^{\rm EM}$.

We rewrite the subtraction term contribution

$$\Delta m_\pi^2(\text{subtr}) = \frac{-3\alpha}{8\pi}\int_0^\infty dQ^2 T_1(-Q^2,0). \tag{82}$$

The subtraction term including the remainder part, except its $O(1/Q^4)$ contributions not present in h_2, is

$$\begin{aligned} T_1(-Q^2,0) = -2 + \frac{2}{F_\pi^2}\int_0^\infty ds\Bigg\{ & \rho_V^R(s)\frac{Q^2}{s+Q^2} \\ & - \rho_A^R(s)\frac{Q^2}{s-p^2+Q^2}\left(1-\frac{p^2}{s}\right) \\ & - g_V(s)\frac{p^2Q^2}{s-p^2+Q^2} + p^2 h_1(p^2,s) \\ & + \frac{p^2 h_2(p^2,s)}{Q^2+f(p^2,s)}\Bigg\}. \end{aligned} \tag{83}$$

We expand the above equation in powers of $1/Q^2$ in order to obtain

$$\begin{aligned} T_1(-Q^2,0) = -2 + \frac{2}{F_\pi^2}\int_0^\infty ds\Bigg[& \rho_V^R(s) - \frac{s-p^2}{s}\rho_A^R(s) \\ & - p^2 g_V(s) + p^2 h_1(p^2,s)\Bigg] \\ & + \int_0^\infty ds\Bigg[s\rho_V^R(s) - \frac{(s-p^2)^2}{s}\rho_A^R(s) \\ & - p^2(s-p^2)g_V(s) + p^2 h_2(p^2,s)\Bigg]\frac{1}{Q^2} \\ & + O\left(\frac{1}{Q^4}\right). \end{aligned} \tag{84}$$

The finiteness of δm_π^2 requires the cancellation of the linear and logarithmic divergences, resulting in the constraints:

$$\begin{aligned} & \int_0^\infty ds\left\{[\rho_V^R(s)-\rho_A^R(s)] + p^2\left[\frac{\rho_A^R(s)}{s} - g_v(s) + h_1(p^2,s)\right]\right\} \\ & \quad = F_\pi^2, \end{aligned} \tag{85}$$

$$\begin{aligned} & \int_0^\infty ds\Bigg\{[s\rho_V^R(s) - s\rho_A^R(s)] + p^2[2\rho_A^R(s) - s g_V(s)] \\ & \qquad + p^4\left[g_V(s) - \frac{\rho_A^R(s)}{s}\right] + p^2 h_2(p^2,s)\Bigg\} = 0. \end{aligned} \tag{86}$$

These constraints also reduce to the Weinberg sum rules when we let $p^2=0$. The role of the functions $h_i(p^2,s)$ (for $i=1, 2$) is to include all other possible contributions. The above constraints must be satisfied exactly, otherwise the pion EM mass difference would be divergent.

We can use the Weinberg sum rules, Eqs. (59) and (60), to further simplify the previous equations:

$$p^2\int_0^\infty ds\left[\frac{\rho_A^R(s)}{s} - g_v(s) + h_1(p^2,s)\right] = 0, \tag{87}$$

$$\begin{aligned} & p^2\int_0^\infty ds\Bigg\{[2\rho_A^R(s) - s g_V(s)] \\ & \quad + p^2\left[g_V(s) - \frac{\rho_A^R(s)}{s}\right] + h_2(p^2,s)\Bigg\} = 0. \end{aligned} \tag{88}$$

We can use solutions available for the functions $\rho_A^R(s)$ [13] and $g_V(s)$ to estimate the integrals for the remainder terms:

$$\begin{aligned} \int_0^\infty ds p^2 h_1(p^2,s) &= \int_0^\infty ds p^2\left[g_v(s) - \frac{\rho_A^R(s)}{s}\right] \\ &= 3.0\times 10^{-4}, \end{aligned} \tag{89}$$

$$\begin{aligned} \int_0^\infty ds p^2 h_2(p^2,s) &= \int_0^\infty ds\Bigg\{p^2[2\rho_A^R(s) - s g_V(s)] \\ &\qquad + p^4\left[g_V(s) - \frac{\rho_A^R(s)}{s}\right]\Bigg\} \\ &= 6.1\times 10^{-4}. \end{aligned} \tag{90}$$

As expected, these values are small when compared to the integrals involving $\rho_V^R(s)$ which are the larger terms in the constraint equations:

$$\int_0^\infty ds\rho_V^R(s) = 3.83\times 10^{-2}, \tag{91}$$

$$\int_0^\infty ds s\rho_V^R(s) = 5.62\times 10^{-2}. \tag{92}$$

The remainder term $R(Q^2,p^2,s)$ allows us to satisfy the constraints exactly since it introduces a small correction to the previous constraint equations. We can proceed to find the subtraction term contribution by following the steps that we used previously in order to obtain Eqs. (44)–(46)

$$\begin{aligned} \Delta m_\pi^2(\text{subtr}) = \frac{-3\alpha}{4\pi F_\pi^2}\int_0^\infty ds\Bigg\{ & \rho_V^R(s) s\ \ln s - \rho_A^R(s)\frac{(s-p^2)^2}{s} \\ & \times\ln(s-p^2) - g_V(s)p^2(s-p^2)\ln(s-p^2) \\ & + p^2 h_2(p^2,s)\ln f(p^2,s)\Bigg\}. \end{aligned} \tag{93}$$

Even though the functions $f(p^2,s)$ and $h_2(p^2,s)$ are undetermined, we have seen in Eq. (90) that their contributions to the constraint Eq. (86) are small.

Numerical result. The total pion electromagnetic mass difference is given by the addition of the elastic term of Eqs. (40), the structure function terms of Eqs. (40) and (78), and

the subtraction constant term of Eq. (93). The results for the narrow-width approximation and for the corresponding spectral functions is given in Table I.

We see from the results that the dominant contribution comes from the subtraction term, which is largely the effect of vector and axial-vector resonances, with modest dependence on $p^2=m_\pi^2$. The elastic term gives the only other significant contribution. The modification because of nonzero width is also not large. The overall result is in excellent agreement with experiment.

TABLE I. $\Delta m_\pi^{\rm EM}$ results.

	Narrow width (MeV)	$\rho_A^R(s),\rho_V^R(s)$ (MeV)
Subtr	4.306	4.124
Elastic	0.500	0.500
Str. Fn. a_1 int. st.	0.028	0.041
Str. Fn. ω int. st.	−0.127	−0.127
Total calculated	4.707	4.538
Experiment	4.594	4.594

V. THE KAON EM MASS DIFFERENCE

Having set up and tested our methodology for the pion, we now proceed to the calculation of the kaon electromagnetic mass difference. The most important effect is that the larger mass of the kaon leads to kinematic corrections in the various formulas. There are also changes in the mass, width and couplings of the resonances which we extract from the data.

The kaon calculation is very similar to the pion one described in the previous section, therefore, we will concentrate on the differences that arise in the kaon case. The kaon counterpart for the Lagrangian of Eq. (20) expanded in terms of kaon, photon, and spin-1 resonance fields is

$$\begin{aligned}\mathcal{L}=&ieA^\mu(K^+\partial_\mu K^- - K^-\partial_\mu K^+)+e^2A^\mu A_\mu K^+K^-\\&-\frac{eF_V}{2}F^{\mu\nu}\left(\rho^0_{\mu\nu}+\sqrt{\frac{2}{3}}\phi_{\mu\nu}+\frac{1}{3}\omega_{\mu\nu}\right)\\&+\frac{eF_V}{4F_K^2}F^{\mu\nu}(\rho^0_{\mu\nu}+\sqrt{2}\phi_{\mu\nu}+\omega_{\mu\nu})K^+K^-\\&+\frac{iG_V}{F_K^2}(\rho^0_{\mu\nu}+\sqrt{2}\phi_{\mu\nu}+\omega_{\mu\nu})\partial_\mu K^+\partial_\nu K^-\\&+\frac{iG_V}{F_K^2}(-\rho^0_{\mu\nu}+\sqrt{2}\phi_{\mu\nu}+\omega_{\mu\nu})\partial_\mu K^0\partial_\nu\overline{K^0}\\&-\frac{ieF_A}{2F_K}F^{\mu\nu}(K_{1\mu\nu}^-K^+-K_{1\mu\nu}^+K^-),\end{aligned}\tag{94}$$

where we have used ideal mixing for the vector-meson resonances.

The major difference between the pion and kaon Lagrangians, Eqs. (20) and (94), respectively, is that in the kaon case all the three nonet vector resonances contribute. Another difference is that there is an elastic contribution to the neutral kaon self-energy. This contribution vanishes in the ideal mixing approximation together with the limit where all the vector resonance masses are equal.

The contribution to the kaon Compton scattering amplitude given by the Feynman diagrams of Figs. 2(a) and 2(b) is

$$\begin{aligned}T_{\mu\nu}^{(1)(K)}(q^2,p\cdot q)=&-2D_{1_{\mu\nu}}+4m_K^2D_{2_{\mu\nu}}\\&\times\{[G_{K^+}(q^2)]^2-[G_{K^0}(q^2)]^2\}\\&\times\left(\frac{1}{m_K^2-(p+q)^2-i\epsilon}+(q\to-q)\right),\end{aligned}\tag{95}$$

where

$$G_{K^+,0}(q^2)\equiv\int_0^\infty du\,\frac{u}{u-q^2}\,\delta_{K^+,0}(u),\tag{96}$$

and

$$\delta_{K^+,0}(u)\equiv\pm\frac{1}{2}\delta(u-m_\rho^2)+\frac{1}{3}\delta(u-m_\phi^2)+\frac{1}{6}\delta(u-m_\omega^2).\tag{97}$$

We have subtracted the neutral kaon contribution in order to be able to use this equation in the following kaon EM mass difference formulas.

The vector sea gull contribution, Fig. 2(c), is

$$T_{\mu\nu}^{(2)(K)}(q^2,p\cdot q)=-2\frac{F_V^2}{F_K^2}\int_0^\infty du\,\frac{q^2}{u-q^2}\,\delta_{K^+}(u)D_{1_{\mu\nu}}.\tag{98}$$

Finally, the axial-vector resonance intermediate state contribution, Fig. 2(d), is

$$\begin{aligned}T_{\mu\nu}^{(3)(K)}(q^2,p\cdot q)=&\frac{F_A^{K^2}}{F_K^2m_{K_1}^2}\,\frac{(p\cdot q+q^2)^2+q^2[m_{K_1}^2-(p+q)^2]}{m_{K_1}^2-(p+q)^2-i\epsilon}+(q\to-q)D_{1\mu\nu}\\&+\frac{F_A^{K^2}}{F_K^2m_{K_1}^2}\left(\frac{-m_K^2q^2}{m_{K_1}^2-(p+q)^2-i\epsilon}+(q\to-q)\right)D_{2\mu\nu}.\end{aligned}\tag{99}$$

The axial-vector intermediate state for the kaon is less straightforward than that for the pion since the axial-vector meson K_1 is an ill-determined mixture of the physical states $K_1(1270)$ and $K_1(1400)$ [34]. We will treat this issue later when we estimate the spectral function for the axial-vector intermediate state.

The breakdown into structure function and subtraction terms of the Compton scattering amplitude given by the above three terms $T_{\mu\nu}^{(i)(K)}$, (for $i=1$–3), in the spectral function representation is

$$T_1(-Q^2,0)=-2+\frac{2}{F_K^2}\int_0^\infty ds\rho_V^K(s)\frac{Q^2}{s+Q^2}-\frac{2}{F_K^2}\int_0^\infty ds\rho_V^K(s)\frac{Q^2}{s-p^2+Q^2}\left(1-\frac{p^2}{s}\right),$$

$$W_1(-Q^2,\nu)=\frac{1}{F_K^2}\int ds\frac{\rho_A^K(s)}{s}(\nu-Q^2)^2\widetilde{K}(\nu,s)\times\delta(s-p^2+Q^2-2\nu), \quad (100)$$

$$W_2(-Q^2,\nu)=4m_K^2\delta(Q^2-2\nu)\times\{[G_{K^+}(-Q^2)]^2-[G_{K^0}(-Q^2)]^2\}+\frac{1}{F_K^2 s}\int ds\frac{\rho_A^K(s)}{s}p^2Q^2\widetilde{K}(\nu,s)\times\delta(s-p^2+Q^2-2\nu),$$

where $\nu=p\cdot q=m_K q_0$, and $p^2=m_K^2$. We have also introduced the convergence factor

$$\widetilde{K}(\nu,s)=\int_0^\infty du\left(\frac{u}{u+2\nu}\right)^4\left(1+\widetilde{\eta}(u)\frac{2\nu}{s}\right)\delta_{K^+}(u), \quad (101)$$

where

$$\widetilde{\eta}(u)=\frac{s}{s-p^2}\left[\left(1+\frac{s-p^2}{u}\right)^4-1\right], \quad (102)$$

and $p^2=m_K^2$.

The definition of the kaon vector spectral function is

$$\rho_V^K(s)\equiv\frac{1}{2}\rho_\rho^R(s)+\frac{1}{2}\rho_\phi^R(s)+\frac{1}{6}\rho_\omega^R(s), \quad (103)$$

where $\rho_\rho^R(s)$ is the spectral function introduced in Fig. 5, and the other two are because of the ϕ and ω intermediate states. For these last two it is appropriate to use the narrow-width approximation.

We also include the VPγ vertices in the same way as we did for the pions. The effective Lagrangian that we use for the $K^*K\gamma$ vertex is

$$\mathcal{L}=e\frac{\sqrt{R_V}}{2}\epsilon^{\mu\nu\alpha\beta}F_{\mu\nu}V_\alpha\partial_\beta K. \quad (104)$$

The subtraction term and structure functions that follow from the above Lagrangian, including the K^0 functions with an extra minus sign to be able to insert them directly in the kaon EM mass difference formula, are

$$T_1(-Q^2,0)=\frac{2}{F_K^2}\int_0^\infty ds g_V^K(s)\frac{p^2Q^2}{s-p^2+Q^2},$$

$$W_1(-Q^2,\nu)=\frac{1}{F_K^2}\int_0^\infty ds g_V^K(s)(\nu^2+p^2Q^2)\widetilde{K}(\nu,s)\times\delta(s-p^2+Q^2-2\nu), \quad (105)$$

$$W_2(-Q^2,\nu)=\frac{1}{F_K^2}\int_0^\infty ds g_V^K(s)p^2Q^2\widetilde{K}(\nu,s)\times\delta(s-p^2+Q^2-2\nu).$$

The narrow-width approximation is justified in this case because of the small width of the K^* intermediate states. Therefore, we use the definition

$$g_V^K(s)\equiv H_{K^{*0}}^2\delta(s-m_{K^{*0}}^2)-H_{K^{*+}}^2\delta(s-m_{K^{*+}}^2). \quad (106)$$

Unlike in the pion case, there is an intermediate vector-meson contribution for the neutral kaon as well as for the charged kaon, in the SU(3) limit. For the pions, the intermediate ρ-meson contribution canceled in the SU(2) limit (since charged and neutral ρ couplings become equal), leaving only the intermediate ω and ϕ contributions to the neutral pion Compton scattering amplitude.

We determine the K^* couplings from the radiative decays $K^*\to K\gamma$,

$$R_{K^{*+}}=\frac{24}{\alpha}\frac{m_{K^{*+}}^3}{(m_{K^{*+}}^2-m_K^2)^3}\Gamma_{K^{*+}\to K^+\gamma}=0.70\pm0.06\ \mathrm{GeV}^{-2},$$

$$R_{K^{*0}}=\frac{24}{\alpha}\frac{m_{K^{*0}}^3}{(m_{K^{*0}}^2-m_K^2)^3}\Gamma_{K^{*0}\to K^0\gamma}=1.61\pm0.14\ \mathrm{GeV}^{-2},$$

from which we obtain the values for

$$H_{K^{*+}}=F_K\sqrt{R_{K^{*+}}}=0.093\pm0.004,$$

$$H_{K^{*0}}=F_K\sqrt{R_{K^{*0}}}=0.143\pm0.006. \quad (107)$$

In the kaon case, the mass difference need not be finite because there can be divergences which are absorbed into the renormalized masses of the up and down quarks. However, this effect is relatively small because it is proportional to αm_u or αm_d compared to the dominant electromagnetic mass shift which is simply of order α. We assume that the renormalization of the up- and down-quark masses has been carried out, although the precise renormalization prescription is hard to define because of the small size of this effect. The remaining electromagnetic effects are finite.

We can now determine the full high Q^2 constraints for a finite kaon EM self-energy given by combining Eqs. (100) and (105), and including the remainder terms introduced in Eq. (81),

TABLE II. $\Delta m_K^{\rm EM}$ results.

	Narrow width (MeV)	$\rho_A^K(s),\rho_V^K(s)$ (MeV)
Subtr	2.56	1.80
Elastic	0.92	0.92
Str. Fn. K_1 int. st.	0.05	0.07
Str. Fn. K^* int. st.	−0.18	−0.18
Total calculated	3.35	2.61
Dashen	1.27	1.27

$$\int_0^\infty ds\left\{[\rho_V^K(s)-\rho_A^K(s)]+p^2x\left[\frac{\rho_A^K(s)}{s}-g_v^K(s)+h_1^K(p^2,s)\right]\right\}=F_K^2, \tag{108}$$

$$\int_0^\infty ds\left\{[s\rho_V^K(s)-s\rho_A^K(s)]+p^2[2\rho_A^K(s)-sg_V^K(s)]+p^4\left[g_V^K(s)-\frac{\rho_A^K(s)}{s}\right]+p^2h_2^K(p^2,s)\right\}=0, \tag{109}$$

where $p^2=m_K^2$. These equations are similar to the ones encountered in the pion case.

Using the above constraints and all available data for the vector spectral function $\rho_V^R(s)$ and the narrow-width approximation for $g_V(s)$, and the ω, ϕ, $\omega(1420)$, $\omega(1600)$, and $\phi(1680)$ resonances, we obtain for $h_1=h_2=0$:

$$\int ds\rho_A^K(s)\left(1-\frac{p^2}{s}\right)=0.0170(12)\ \text{GeV}^2, \tag{110}$$

$$\int dss\rho_A^K(s)\left(1-\frac{p^2}{s}\right)^2=0.0406(16)\ \text{GeV}^4, \tag{111}$$

where $p^2=m_K^2$.

We try first the narrow-width approximation to the axial-vector spectral function

$$\rho_A^{K(\rm NW)}(s)=F_{A\,(\rm NW)}^{K2}[\cos^2\theta_K\delta(s-m_{K_1(1400)}^2)+\sin^2\theta_K\delta(s-m_{K_1(1270)}^2)+R_K^2\delta(s-m_{K_1(HR)}^2)]. \tag{112}$$

This parametrization includes the $K_1(1270)$ and $K_1(1400)$ resonances as well as a higher mass resonance $K_1(HR)$. The input parameters to ρ_A^K for this calculation are

$$\theta_K=\frac{\pi}{4}\quad\text{and}\quad m_{K_1(HR)}=2.0\ \text{GeV}. \tag{113}$$

These choices are sensible but arbitrary. They fix the values of F_A^K and R_K through the constraint equations (110) and (111). The obtained values for F_A^K and R_K show a sizable dependence on the choice of $m_{K_1(HR)}$. The results for the different contributions to $\delta m_K^{\rm EM}$ obtained by this narrow-width approximation are given in Table II. In particular, we find that the subtraction term contribution is very large.

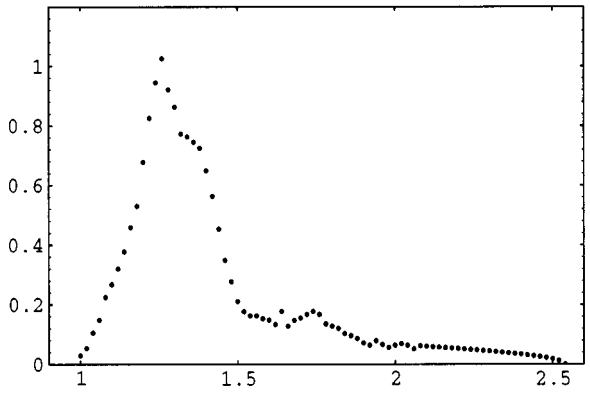

FIG. 7. $\overline{\rho_A}(s)$ vs $m_{K\pi\pi}$ (GeV).

However, this contribution varies from $\delta m_K^{(\rm subtr)}\sim 2.3$ MeV for $m_{K_1(HR)}=1.8$ GeV to $\delta m_K^{(\rm subtr)}\sim 3.1$ MeV for $m_{K_1(HR)}=2.4$ GeV. These numerical results only constitute a very rough estimate. This is already indicated by the large dependence in $m_{K_1(HR)}$ and, once again, it involves the narrow-width approximation for broad resonances.

There is another constraint on the axial-vector spectral function because of τ decay:

$$B(\tau\to\nu_\tau K_1\to\nu_\tau K\pi\pi)=E_\tau\int_0^{m_\tau^2}ds\rho_A^K(s)\left(1-\frac{s}{m_\tau^2}\right)^2\times\left(1+\frac{2s}{m_\tau^2}\right), \tag{114}$$

where

$$E_\tau=\frac{G_\mu^2m_\tau^3|V_{us}|^2}{8\pi\Gamma_\tau}=0.6633\ \text{GeV}^{-2}. \tag{115}$$

The data for the τ lepton decay, $\tau\to\nu_\tau K\pi\pi$, gives the branching ratios [35],

$$B(\tau^-\to\nu_\tau K^-\pi^+\pi^-)=(0.40\pm0.09)\%, \tag{116}$$

$$B(\tau^-\to\nu_\tau\overline{K^0}\pi^-\pi^0)=(0.41\pm0.07)\%, \tag{117}$$

$$B(\tau^-\to\nu_\tau K^-\pi^0\pi^0)=(0.09\pm0.03)\%, \tag{118}$$

$$B(\tau\to\nu_\tau K\pi\pi)=(0.90\pm0.12)\%. \tag{119}$$

The last branching ratio is the sum of the three different decay channels with the uncertainties added in quadrature. Even though we expect these branching ratios to be dominated by the axial-vector channels, especially the $K_1(1270)$ and the $K_1(1400)$, there should also be a contribution because of the vector resonance $K^*(1410)$ [36]. This resonance will contribute through the decay process $K^*(1410)\to K^*(892)\pi\to K\pi\pi$. The branching ratio for $K^*(1410)\to K^*(892)\pi$ is greater than 40% at 95% confidence level [34], and $B[K^*(892\to K\pi)]\sim 100\%$. Therefore, the τ branching ratio into the strange axial-vector channels should be somewhat lower than stated in Eq. (119).

We obtain the shape of $\rho_A^K(s)$, up to $m_{K\pi\pi}=2.1$ GeV, from diffractive production experimental data obtained by

the ACCMOR Collaboration in 1981 [37]. The data was extracted from 200 000 examples of the reaction $K^- p \to K^- \pi^- \pi^+ p$. The intensity for the 1^+ channel gives us the shape of $\rho_A^K(s)$.

We add a high energy tail to the data, up to $m_{K\pi\pi}=2.54$ GeV, which decreases quadratically. The constraint equations favor this quadratic choice instead of other simple parametrizations. The final normalization of the spectral function is obtained by enforcing the constraint equations (110) and (111). If we define

$$\rho_A^K(s) \equiv F_A^{K^2} \overline{\rho_A}(s), \text{ where } \int ds \overline{\rho_A}(s) = 1, \qquad (120)$$

we obtain $F_A^K = 0.144$ GeV, and the $\overline{\rho_A}(s)$ given in Fig. 7.

The choice of ρ_A^K results in an estimate for the τ branching ratio for the $K^*(1410)$ vectorial resonance,

$$B[\tau \to \nu_\tau K^*(1410)] = (0.46 \pm 0.13)\%. \qquad (121)$$

This value could be extracted from data by doing an angular momentum analysis of the $K\pi\pi$ final state.

The final results for the different contributions to Δm_K are given in Table II. We estimate the uncertainty of the total kaon EM mass difference to be $\sigma(\Delta m_K) \sim 0.6$ MeV.

Our result is about 100% greater than Dashen's result. This result is in better agreement with earlier Refs. [3,5,38], and with the recent investigation [4], but in disagreement with Baur and Urech [2]. Given the uncertainty of our result, we feel more comfortable by saying that we find a modification of Dashen's theorem between 160% and 240% .

VI. CONCLUSIONS

The calculation of nonleptonic amplitudes is in general one of the most difficult tasks for analytic strong interaction techniques. The elecromagnetic mass differences of the pseudoscalar mesons seems to us to be the most favorable case to attempt a controlled calculation. There turn out to be several favorable circumstances that help in this endeavor. As we have exploited above, the relevant current-current products have several connections to known phenomenology, and have important constraints because of the long-distance chiral behavior and the short-distance properties of QCD.

The calculation of the known pion mass difference was quite successful. It turns out that intermediate mass scales (around 1 GeV) are the most important for this matrix element, and these are well represented by resonance contributions. In fact, this structure is already visible in the old calculation in the soft-pion limit given by Das *et al.* where the vector and axial-vector spectral functions determine the mass difference in the chiral limit. There are calculable corrections and even new diagrams that come in as one includes a nonzero pion mass, but the pion mass is still small enough that one does not change the general anatomy of the matrix element.

In the case of the kaon mass difference, the experimental result is not known. We find a large deviation from the prediction of Dashen's theorem, which is valid in the limit of massless kaons. While the magnitude of this effect is larger than most SU(3)-breaking effects in chiral calculations, we stress that its origin is in reasonably well-known and mundane effects, and does not represent any breakdown of chiral symmetry. The main effect seems to be the kaon mass in the propagator of the Born diagram which, hence, is a rather long-distance effect, while the remaining dependence comes from the known shift in resonance masses because of the strange quark mass. This mass difference is important for the extraction of the $u-d$ quark mass difference.

ACKNOWLEDGMENTS

We would like to thank the U.S. Department of Energy (Grant No. DE-FG02-84ER40153) and the National Science Foundation for providing the funds that supported this work.

APPENDIX

The notation used for the $O(E^2)$ chiral terms in the Lagrangian of Eq. (19) is

$$U = \exp(i\sqrt{2}\Phi/F),$$

$$\Phi = \begin{pmatrix} \frac{\pi^0}{\sqrt{2}} + \frac{\eta_8}{\sqrt{6}} & \pi^+ & K^+ \\ \pi^- & -\frac{\pi^0}{\sqrt{2}} + \frac{\eta_8}{\sqrt{6}} & K^0 \\ K^- & \overline{K^0} & -\frac{2}{\sqrt{6}}\eta_8 \end{pmatrix},$$

$$\chi = 2B_0 \begin{pmatrix} m_u & 0 & 0 \\ 0 & m_d & 0 \\ 0 & 0 & m_s \end{pmatrix},$$

$$D_\mu U = \partial_\mu U - i(v_\mu + a_\mu)U + iU(v_\mu - a_\mu), \qquad (A1)$$

where v^μ, a^μ are the external fields. In order to include EM one needs to define

$$a_\mu = 0, \quad v_\mu = eQA_\mu, \qquad (A2)$$

where A_μ is the photon field, and should not be confused with the axial-vector antisymmetric tensor field which has two Lorentz indices, $A_{\mu\nu}$. Q is the quark charge matrix, for the u, d, and s quarks,

$$Q = \begin{pmatrix} \frac{2}{3} & 0 & 0 \\ 0 & -\frac{1}{3} & 0 \\ 0 & 0 & -\frac{1}{3} \end{pmatrix}. \qquad (A3)$$

The notation used for Lagrangian containing the chiral couplings of the vector and axial-vector-meson resonances, Eq. (19), is

$$u_\mu = iu^\dagger D_\mu U u^\dagger = u_\mu^\dagger,$$

$$f_\pm^{\mu\nu} = uF_L^{\mu\nu}u^\dagger \pm u^\dagger F_R^{\mu\nu}u,$$

$$F_{R,L}^{\mu\nu} = \partial^\mu(v^\nu \pm a^\nu) - \partial^\nu(v^\mu \pm a^\mu) - i[v^\mu \pm a^\mu, v^\nu \pm a^\nu],$$

$$V_{\mu\nu}=\begin{pmatrix} \frac{\rho^0}{\sqrt{2}}+\frac{\omega_8}{\sqrt{6}} & \rho^+ & K^{*+} \\ \rho^- & -\frac{\rho^0}{\sqrt{2}}+\frac{\omega_8}{\sqrt{6}} & K^{*0} \\ K^{*-} & \overline{K^{*0}} & -\frac{2}{\sqrt{6}}\omega_8 \end{pmatrix}_{\mu\nu},$$

$$A_{\mu\nu}=\begin{pmatrix} \frac{a_1^0}{\sqrt{2}}+\frac{f_1}{\sqrt{6}} & a_1^+ & K_1^+ \\ a_1^- & -\frac{a_1^0}{\sqrt{2}}+\frac{f_1}{\sqrt{6}} & K_1^0 \\ K_1^- & \overline{K_1^0} & -\frac{2}{\sqrt{6}}f_1 \end{pmatrix}_{\mu\nu}, \quad \text{(A4)}$$

$$\nabla_\lambda R_{\mu\nu}=\partial_\lambda R_{\mu\nu}+[\Gamma_\lambda, R_{\mu\nu}],$$

$$R_{\mu\nu}=V_{\mu\nu}, A_{\mu\nu},$$

$$\Gamma_\mu=\frac{1}{2}\{u^\dagger[\partial_\lambda-i(v_\lambda+a_\lambda)]u+u[\partial_\lambda-i(v_\lambda-a_\lambda)]u^\dagger\}. \quad \text{(A5)}$$

From the kinetic terms of the Lagrangian in Eq. (19) one derives the free propagator for the antisymmetric tensor field representation [24],

$$\langle 0|TR_{\mu\nu}(x)R_{\rho\sigma}(y)|0\rangle=\frac{-i}{M^2}\int\frac{d^4k}{2\pi^4}\frac{e^{-i(x-y)}}{M^2-k^2-i\epsilon}\times[g_{\mu\rho}g_{\nu\sigma}(M^2-k^2)+g_{\mu\rho}k_\nu k_\sigma-g_{\mu\sigma}k_\nu k_\rho-(\mu\leftrightarrow\nu)], \quad \text{(A6)}$$

where the normalization is given by

$$\langle 0|R_{\mu\nu}|R(\epsilon,p)\rangle=\frac{-i}{M}[p_\mu\epsilon_\nu(p)-p_\nu\epsilon_\mu(p)]. \quad \text{(A7)}$$

[1] W. A. Bardeen, J. Bijnens, and J.-M. Gérard, Phys. Rev. Lett. **62**, 1343 (1989).
[2] R. Baur and R. Urech, Phys. Rev. D **53**, 6552 (1996).
[3] J. Bijnens, Phys. Lett. B **306**, 343 (1993).
[4] J. Bijnens and J. Prades, Nucl. Phys. B (to to be published).
[5] J. F. Donghue, B. R. Holstein, and D. Wyler, Phys. Rev. D **47**, 2089 (1993).
[6] J. F. Donoghue, in *The Building Blocks of Creation: From Microfermi's to Megaparsecs*, Proceedings of the Theoretical Advanced Study Institute, Boulder, Colorado, edited by S. Raby and T. Walker (World Scientific, Singapore, 1994), hep-ph/9610360.
[7] J. Gasser and M. Leutwyler, Phys. Rep. **87**, 77 (1982).
[8] H. Leutwyler, Phys. Lett. B **378**, 313 (1996).
[9] R. Dashen, Phys. Rev. **183**, 1245 (1969).
[10] A. Duncan, E. Eichten, and H. Thacker, Phys. Rev. Lett. **76**, 3894 (1996).
[11] J. Gasser and H. Leutwyler, Ann. Phys. (N.Y.) **158**, 142 (1984).
[12] J. Gasser and H. Leutwyler, Nucl. Phys. **B250**, 465 (1985).
[13] J. F. Donoghue and E. Golowich, Phys. Rev. D **49**, 1513 (1994).
[14] J. Bijnens and F. Cornet, Nucl. Phys. **B296**, 557 (1988).
[15] J. F. Donoghue, B. R. Holstein, and Y. Lin, Phys. Rev. D **37**, 2423 (1988).
[16] J. F. Donoghue and B. R. Holstein, Phys. Rev. D **40**, 3700 (1989).
[17] J. F. Donoghue and B. R. Holstein, Phys. Rev. D **48**, 137 (1993).
[18] R. Urech, Nucl. Phys. **B433**, 234 (1995).
[19] Riazuddin, Phys. Rev. **114**, 1184 (1959).
[20] R. H. Socolow, Phys. Rev. **137**, B1221 (1965).
[21] T. Das *et al.*, Phys. Rev. Lett. **18**, 759 (1967).
[22] S. Weinberg, Phys. Rev. Lett. **18**, 507 (1967).
[23] P. Ko, Phys. Rev. D **41**, 1531 (1990).
[24] G. Ecker *et al.*, Nucl. Phys. **B321**, 311 (1989).
[25] G. Ecker *et al.*, Phys. Lett. B **223**, 425 (1989).
[26] G. Barton, *Dispersion Techniques in Field Theory* (Benjamin, New York, 1965).
[27] J. D. Bjorken and S. D. Drell, *Relativistic Quantum Fields* (McGraw-Hill, New York, 1965).
[28] W. N. Cottingham, Ann. Phys. (N.Y.) **25**, 424 (1963).
[29] S. L. Adler and R. Dashen, *Currnt Algebras and Applications to Particle Physics* (Benjamin, New York, 1968).
[30] J. D. Bjorken, Phys. Rev. **179**, 1547 (1969).
[31] A. F. Pérez, Ph.D. thesis, University of Massachusetts, Amherst, 1995.
[32] P. J. O'Donnell, Rev. Mod. Phys. **53**, 673 (1981).
[33] K. Tanaka, Phys. Rev. **133**, B1540 (1964).
[34] Particle Data Group, L. Montanet *et al.*, Phys. Rev. D **50**, 1173 (1994).
[35] B. K. Heltsley, Nucl. Phys. **B250**, 539 (1985).
[36] D. Aston *et al.*, Nucl. Phys. **B202**, 21 (1982).
[37] ACCMOR Collaboration, C. Daum *et al.*, Nucl. Phys. **B187**, 1 (1981).
[38] J. Gasser and H. Leutwyler, Nucl. Phys. **B250**, 539 (1985).